

LUT UNIVERSITY
LUT School of Energy Systems
LUT Mechanical Engineering

Väinö Friman

**BENEFITS OF DYNAMIC FINITE ELEMENT ANALYSIS FOR ELEVATOR
BUFFER EXTENSION STRUCTURE DESIGN**

Examiner(s): Professor Timo Björk

M. Sc. (Tech.) Marco Guglielmo

TIIVISTELMÄ

LUT-Yliopisto
LUT School of Energy Systems
LUT Kone

Väinö Friman

Benefits of dynamic finite element analysis for elevator buffer extension structure design

Diplomityö

2022

63 sivua, 38 kuvaa ja 12 taulukkoa

Tarkastajat: Professori Timo Björk
DI Marco Guglielmo

Hakusanat: Dynamiikka, elementtimenetelmä, hissi, törmäysvaimennin

Tämä diplomityö tehtiin suomalaiselle hissivalmistajalle KONE. Työ keskittyi tarkastelemaan hissi-törmäysvaimenninrakenteiden kestävyyttä. Tavoitteena työssä oli varmentaa käytössä oleva tapa arvioida kuormitusta staatisessa analyysissä, koska törmäysvaimentimia käsittelevät standardit eivät ohjeista miten kuormitus tulee laskea. Tavoitteena oli myös tarkastella, olisiko dynaamisesta analyysistä lisähyötyä rakenteiden tarkastelussa, koska törmäyskuormitus on ilmiönä erittäin nopea. Lisäksi haluttiin löytää mahdollinen tapa tarkastella korkempia törmäysnopeuksia kuin määrätty 1.0 m/s nopeus.

Tutkimus suoritettiin ensiksi kokoamalla vertailudataa kokeellisista testeistä, jotka suoritettiin EN 81-50 mukaan kolmella eri törmäysnopeudella. Testit suoritettiin yhdelle törmäysvaimenninrakenteelle kahdella eri ylälevykonfiguraatiolla, heikommalla ja vahvemmallalla levyllä. Tämän jälkeen suoritettiin numeeriset analyysit staatisella elementtimenetelmällä ja eksplisiittisellä dynaamisella elementtimenetelmällä, käyttäen erilaisia tapoja arvioida kuormitusta. Staatisessa analyysissä käytettiin kolmea eri kuormitustapaa, joista ensimmäinen oli törmäyskerroinkuormitus, joka johdettiin EN 81-20 ja EN 81-50 standardeista. Staattisen analyysin kaksi muuta kuormitusta kerättiin kokeellisesta datasta, nämä olivat absoluuttinen maksimikuormitus ja keskiarvoinen kuormitus 40 ms aikavälillä. Dynaaminen analyysi suoritettiin massaimpaktina ensiksi pelkällä alkunopeudella sekä myös kuormituksella, jossa massa vaikuttaa alkunopeus ja normaali putoamiskiihtyvyys. Tärkein tarkastelukriteeri oli plastiset muodonmuutokset.

Tuloksia verrattiin kokeelliseen dataan ylälevyjen deformaatioiden ollessa tärkein tarkastelun kohde. Tulosten perusteella voitiin todeta, että staattinen analyysi on validi törmäyskerroinkuormituksella 1.0 m/s impakteissa. Myös dynaaminen analyysi alkunopeudella sekä putoamiskiihtyvyydellä todettiin hyödylliseksi ainakin korkeintaan 1.75 m/s impakteissa. Tämän lisäksi pystyttiin antamaan kehitysehdotuksia analyysitarkkuuden parantamiseen.

ABSTRACT

LUT Univeristy
LUT School of Energy Systems
LUT Mechanical Engineering

Väinö Friman

Benefits of dynamic finite element analysis for elevator buffer extension structure design

Master's thesis

2022

63 pages, 38 figures and 12 tables.

Examiners: Professor Timo Björk
M. Sc. (Tech.) Marco Guglielmo

Keywords: Dynamic, finite element analysis, elevator, buffer

This master's thesis was done for Finnish elevator manufacturer KONE. The thesis focused on evaluating structural integrity of elevator buffer extension structures. The goal was to evaluate currently used method of estimating impact loading in static finite element analysis, because the standards concerning impact buffers do not include instructions for estimating the loading for structural analysis. Additional goal was to find out if dynamic analysis would be needed because of the rapid nature of the phenomena. KONE also wanted to find out a possible way to estimate loading in higher speed impacts than the rated speed of 1.0 m/s.

The research was carried out by firstly creating reference data with experimental tests including one type of buffer extension structure with two different buffer plate configurations, one weaker plate and one stronger plate. The experimental tests were carried out as drop tests according to EN 81-50 standard with three different impact speeds. Secondly numerical analysis of the structure was carried out with static and explicit dynamic finite element analyses with different load cases estimating the impact loading. For static analysis three load cases were used, firstly an impact factor load was derived from the EN 81-20 and EN 81-50 standards. In addition to this, two loading cases for static analysis were created with the drop test data, an absolute maximum loading during the test and the largest average over 40 ms time interval. Dynamic analysis was carried out with two types of a mass impacts first only with initial velocity of the mass and then with initial velocity and standard earth gravity affecting the system. The main evaluation criterion was plastic deformation.

Results of the numerical analysis methods were compared to the experimental data with deformations in the buffer plates being the main point of focus. With these results the static impact factor loading could be validated for 1.0 m/s impacts. Dynamic analysis including initial velocity and gravity proved to be beneficial in evaluating impacts with speeds up to 1.75 m/s. In addition to this, good propositions for increasing the analysis accuracy were given.

ACKNOWLEDGEMENTS

Special thanks go firstly to KONE for providing the interesting topic of the thesis and to Marco Guglielmo for supervising the work. Secondly, I want to thank Professor Timo Björk for guidance during the process and D.Sc. (Tech) Antti Ahola for support in modelling work. Koneenrakennuskilta has been a huge part of my life during my time in Lappeenranta, and I want to also thank all current and former members for creating a great atmosphere to learn and to bond with. Huge thanks go also to my friends and family for providing a stable foundation during my studies. University studies have been a long and even at sometimes grueling part of my life giving many unforgettable memories. However, everything great has an ending, and I am looking forward to the challenges ahead. Afterall I am grateful for all the experiences and friends I gained.

Väinö Friman

Riihimäki 24.8.2022

TABLE OF CONTENTS

TIIVISTELMÄ

ABSTRACT

ACKNOWLEDGEMENTS

TABLE OF CONTENTS

LIST OF SYMBOLS AND ABBREVIATIONS

1	INTRODUCTION	9
2	BACKGROUND	11
	2.1 Impact buffers for elevator shafts	11
	2.2 Elevator safety equipment standards	11
	2.3 Buffer assembly	12
	2.4 Analytical model of the phenomena	16
	2.5 Scope.....	18
3	METHODS.....	19
	3.1 Drop test.....	19
	3.2 Static FE-analysis	20
	3.3 Explicit dynamic FE-analysis	21
4	IMPLEMENTATION OF METHODS	23
	4.1 Drop test parameters	23
	4.2 Material models for FE-analysis.....	23
	4.3 Static FE-models.....	27
	4.4 Dynamic FE-models	30
5	RESULTS	32
	5.1 Drop test results	32
	5.2 Static FE-analysis results	35
	5.3 Dynamic FE-analysis results	40
6	ANALYSIS & DISCUSSION	47
	6.1 Result comparison.....	47
	6.2 Applicability to buffer extension design.....	54
	6.3 Reliability, validity and sensitivity aspects.....	56
	6.4 Suggestions for improvements.....	58

7 CONCLUSIONS.....60
LIST OF REFERENCES.....62

LIST OF SYMBOLS AND ABBREVIATIONS

A	Initial buffer area [mm ²]
c_{PU}	Damper coefficient of polyurethane
D	Plate diameter [mm]
D_{PU}	Buffer diameter [mm]
E_{PU}	Young's modulus for polyurethane [MPa]
E_{S}	Young's modulus for steel [MPa]
e	Energy [J]
F	Force [N]
f_{u}	Ultimate strength of steel [MPa]
f_{y}	Yield strength of steel [MPa]
G	Shear modulus [MPa]
g	Acceleration due to earth gravity [m/s ²]
g_{n}	Acceleration due to earth gravity in EN 81-20 [m/s ²]
H_{PU}	Buffer height [mm]
$h_{1.0}$	1.0 m/s impact speed drop height [mm]
$h_{1.75}$	1.75 m/s impact speed drop height [mm]
$h_{2.5}$	2.5 m/s impact speed drop height [mm]
i	Impact factor
K	Bulk modulus [MPa]
k_{PU}	Spring constant of polyurethane [N/mm]
k_{S}	Spring constant of steel [N/mm]
m	Mass [kg]
m_0	Initial mass [kg]
T	Plate thickness [mm]
t	Time [s]
t_0	Initial time [s]
V	Volume [mm ³]
V_0	Initial volume [mm ³]
ν	Impact speed [m/s]
ν_{PU}	Poisson's value for polyurethane

ν_s	Poisson's value for steel
v_0	Initial speed [m/s]
x	Height of falling object [mm]
x_0	Initial height of falling object [mm]
y_{PU}	Displacement of polyurethane [mm]
y_s	Displacement of steel [mm]
\dot{y}	Speed [m/s]
\ddot{y}	Acceleration [m/s ²]
\dddot{y}	Jerk [m/s ³]
ε	Strain
$\varepsilon_{\text{engineering}}$	Engineering strain
$\varepsilon_{\text{true}}$	True strain
ε_u	Ultimate strain of steel
ε_y	Yield strain of steel
ρ	Density [kg/m ³]
ρ_0	Initial density [kg/m ³]
σ	Stress [MPa]
$\sigma_{\text{engineering}}$	Engineering stress [MPa]
σ_{true}	True stress [MPa]
FE	Finite element
PU	Polyurethane
RHS	Rectangular hollow section

1 INTRODUCTION

This thesis was done for Finnish elevator manufacturer KONE. The research focused on comparing the benefits of a dynamic finite element (FE)-analysis to currently used static FE-analysis, when applied in elevator buffer extension structure design.

Impact buffers placed under the elevator car and the counterweights are used according to EN 81-20 standard which determines 1.0 m/s as the maximum speed at which the buffers can be used. The problem with this standard is that it doesn't include precise instructions for calculating design loads for buffer structures. The EN 81-50 standard only provides the requirements for buffers which need to be fulfilled, the same requirements also apply for the extension structure of the buffers, but no additional calculation guidelines are given. KONE desires to also have a method to evaluate buffers for higher speed impacts than the rated speed to account for worst-case scenario situations. The motivation for KONE was to evaluate the currently used static FE-method and to find the best possible method for analyzing the different impacts speeds.

The goal of this thesis was to experiment the utilization of static FE-analysis and dynamic FE-analysis to find a more efficient way to simulate impact loading in a buffer structure. The main questions were to find out if dynamic analysis was needed because of the nature of the impact phenomena is happening very rapidly or was the currently used static FE-method valid. In addition to this a second question was to find out if a good method of evaluating higher impact speeds than the standard 1.0 m/s could be created. Generally, the assumption was that if dynamic analysis would prove to be accurate in depicting behavior in buffer impacts, it could be very useful in designing new buffer extension structures and help evaluate the structural integrity of existing buffer types. The benefit of dynamic analysis would be that no additional calculations for predicting the impact loading would need to be done. However, the possible downside of dynamic analysis is inevitably the substantially increased solving time compared to the static analysis.

The research of the thesis was done by creating different types of static FE-models which were created with different ways to predict the impact loading of the structure. These were compared to dynamic FE-models in which the simulation of loading is based on simple physics, which means that by simply simulating a mass impacting the structure as loading is applied to the system. The evaluation of the numerical methods was done by comparing the results to each other and to experimental buffer drop test data.

The main evaluation criteria of the methods were deformations in the structure. By comparing the deformation results of all the different methods to the drop test results the best methods for evaluating different impact speeds in buffer impacts were proposed. The applicability of these methods was also discussed and the validity of the results they provide were assessed. Lastly, some suggestions for improving the method accuracy were given.

2 BACKGROUND

This chapter defines all important background information regarding the thesis. Relevant standards for the topic are covered only from the point of view regarding buffers with non-linear characteristics. The physical phenomenon is explained analytically, the assembly of the evaluated buffer is presented and the scope for the thesis is defined.

2.1 Impact buffers for elevator shafts

Elevators today are required to have many different safety equipment preventing accidents originating from overrun, overspeed and free fall situations to elevator users or goods. Impact buffers placed in the elevator shaft under the elevator car and the counterweights are the last piece of safety equipment helping to absorb the impact in case of all else safety equipment has failed. Before the buffer impact can happen, the elevator would first need to miss the last landing stop, or the brakes and after that the overspeed governor connected to the safety gear both would need to fail to function. (Lozzi & Briozzo 2000, p. 323-325.) In this situation the impact buffers will absorb the impact helping to mitigate any serious damages to personnel or goods inside the elevator car (Mirables, Cuartero & Castejon 2013, p. 1). This thesis focuses on a situation in which a counterweight hits the impact buffer with the rated speed of 1.0 m/s and with speeds higher than that, with the purpose of finding efficient ways to predict stresses and deformations in the buffer extension structures.

2.2 Elevator safety equipment standards

Elevator technology has been developing very fast since the very first elevators were designed and the safety standards regarding this technology are updated frequently (Thilmany 2013, p. 49). The necessary safety standards for this research are the ones which define safety requirements and design and calculation policies of impact buffers in Europe. EN 81-20 standard defines the safety rules for safeguarding persons and objects under normal operation procedures. The standard describes the design requirements for buffers with nonlinear characteristics, which are the types of buffers in question in this thesis. The requirements are mainly bound to multiples of standard earth gravity g_n .

According to EN 81-20, 2020 Chapter 5.8.2.1.2.1: “Energy accumulation type buffers with nonlinear characteristics shall fulfil the following requirements when hitting the buffer(s) with the mass of the car and its rated load or of the counterweight, in case of free fall with speed of 115% of the rated speed:

- a) the retardation according to EN 81-50:2020, 5.5.3.2.6.1 a) shall not be more than $1g_n$;
- b) retardation of more than $2.5g_n$ shall not be longer than 0.04 s;
- c) the return speed of the car of the counterweight shall not exceed 1 m/s;
- d) there shall be no permanent deformation after actuation.
- e) the maximum peak retardation shall not exceed $6g_n$.” (EN 81-20 2020, p. 95)

The EN 81-20 standard refers also to EN 81-50 standard, which is also essential in this thesis work. It defines design rules, calculations, examinations and tests of specific lift components. EN 81-50 standard includes testing and calculation instructions in chapter 5.5.3.2. Energy accumulation buffers with nonlinear characteristics. The experimental buffer drop test was done according to these instructions with the exemption of additional higher test speeds. The chapter states the most essential design criteria for buffers in chapter 5.5.3.2.6.2: “After the tests with the maximum mass no part of the buffer shall show any permanent deformation or be damaged so that its condition shall guarantee normal operation.” (EN 81-50 2020, p. 27)

These standards do not include precise instructions for calculating the design loads for buffer evaluation they only determine the criteria for validating these designs and set the limitations for buffer manufactures to meet. Therefore, one of the objectives of this thesis was to demonstrate a valid method for these calculations.

2.3 Buffer assembly

KONE has many different buffer extension designs for different applications. For this research the most challenging buffer in terms of structural integrity was chosen. With this, the findings should be the easiest to implement to the other buffer types also. The buffer chosen for examination is an adjustable buffer which has an easy setting for on-site adjustments of the final height. This is possible with a threaded rod that changes the height of the buffer plate. In Figure 1 is presented the analyzed buffer extension structure, the

polyurethane (PU)-buffer is fixed on top of the plate with a screw going through the plate and connecting to the adjustment rod.



Figure 1. Buffer assembly.

The assembly consists of a bottom plate, a rectangular hollow section (RHS)-beam, a threaded top plate of the beam, a M24 nut, an adjustment rod, a buffer plate and a polyurethane buffer. The top plate and the bottom plate are welded to the RHS-beam with a fillet weld which has 3 mm throat thickness. Figure 2 shows the polyurethane buffer which is fixed on top of the extension structure. The buffer dimensions are height $H_{PU} = 80$ mm, diameter $D_{PU} = 125$ mm.



Figure 2. PU-buffer.

The extension structure was tested with two different plate configurations, named for this thesis as a strong plate and a weak plate. The strong plate is a steel plate with thickness $T = 10$ mm and the weak plate is two 5 mm thick plates welded together with fillet weld which has 3 mm throat thickness. The overall diameter D of both plates is 130 mm. These buffer plates are presented in Figure 3 and Figure 4.

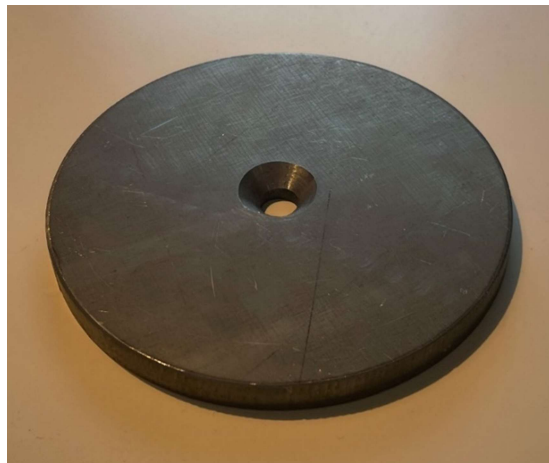


Figure 3. Strong plate, $T = 10$ mm, $D = 130$ mm.

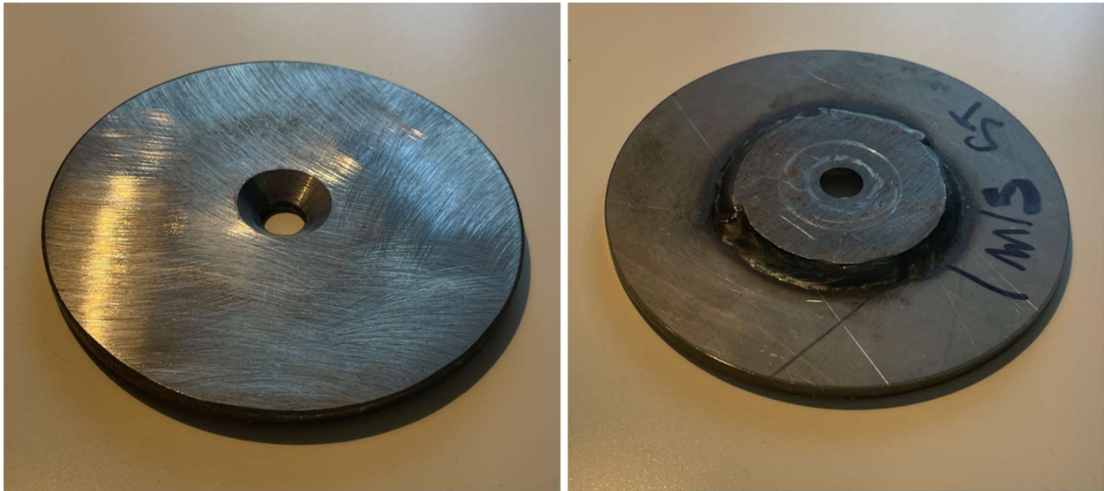


Figure 4. Weak plate from top and bottom. Top plate $D = 130$ mm, bottom plate $D = 60$ mm, both plates $T = 5$ mm.

Material for the steel parts of the assembly is S355 structural steel. Material of the buffer is a polyurethane elastomer, manufacturer provided following force-deflection diagrams presented in Figure 5 and Figure 6.

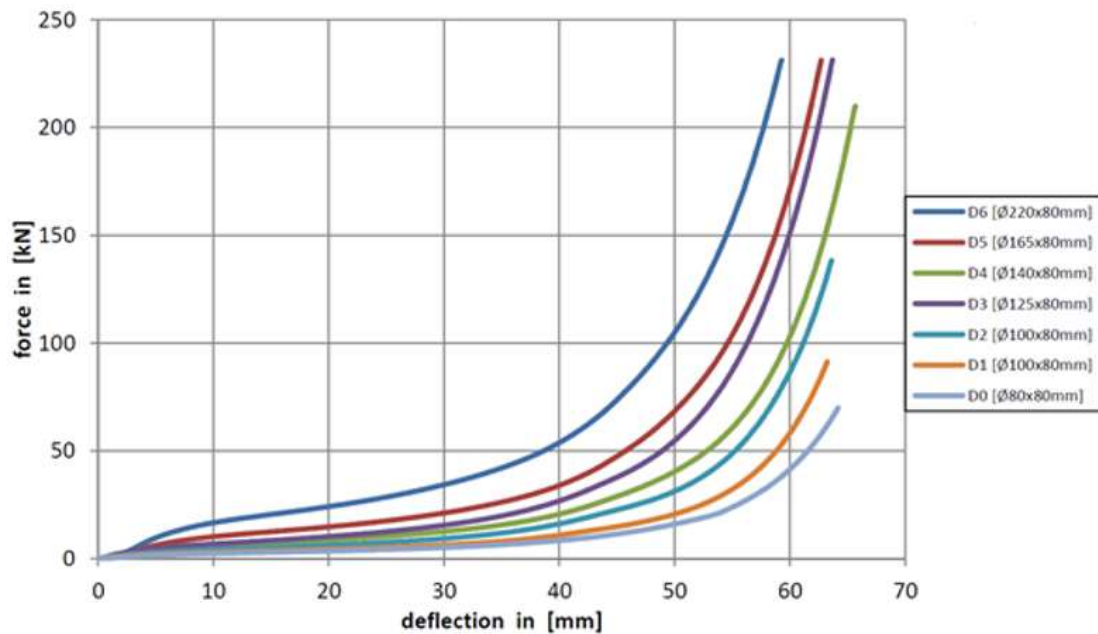


Figure 5. Force deflection diagram for the PU buffer, inspected buffer type D3.

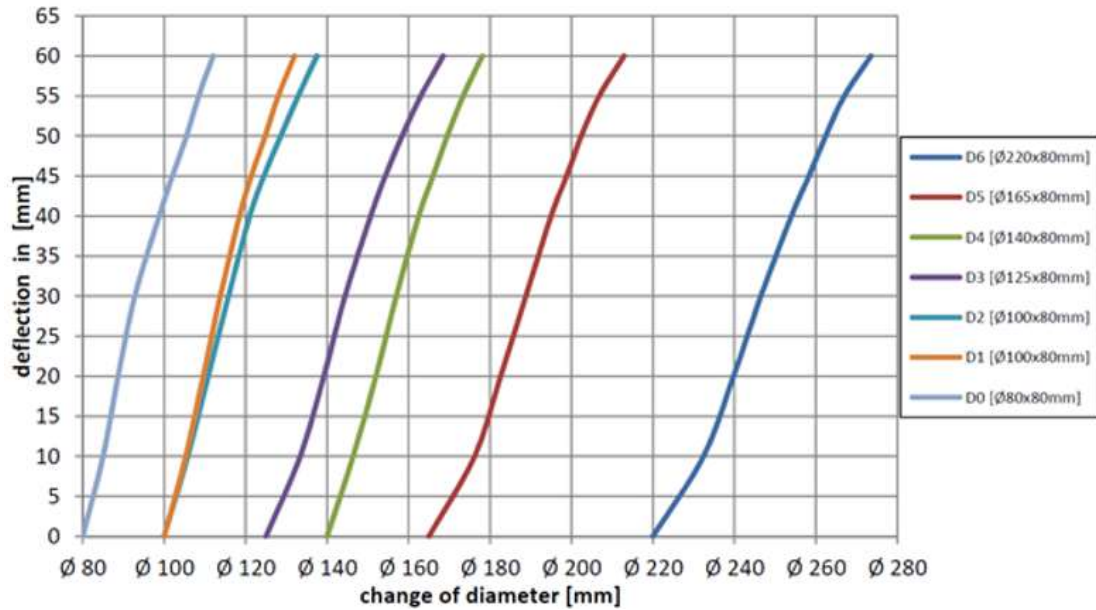


Figure 6. Transverse strain at deflection for the PU buffer, inspected buffer type D3.

2.4 Analytical model of the phenomena

Analytically the physical phenomena of a buffer impact can be expressed as an impact force loading $m\dot{y}$ at point of time t , induced by mass m impacting the buffer with speed \dot{y} . This will induce a displacement y to the system which is the result of the viscoelastic deformation of the PU-buffer and the elasticity of the steel structure. Viscoelastic behavior of the PU buffer can be represented as displacement y_{PU} , speed $c_{PU}\dot{y}_{PU}$ with damper coefficient c_{PU} and elasticity as spring constant k_{PU} . The dynamic behavior of the steel structure can be defined as displacement of a spring y_S with spring constant k_S . The combined dynamic behavior of the assembly can be represented by a Maxwell model and a spring model in a series, presented in Figure 7.

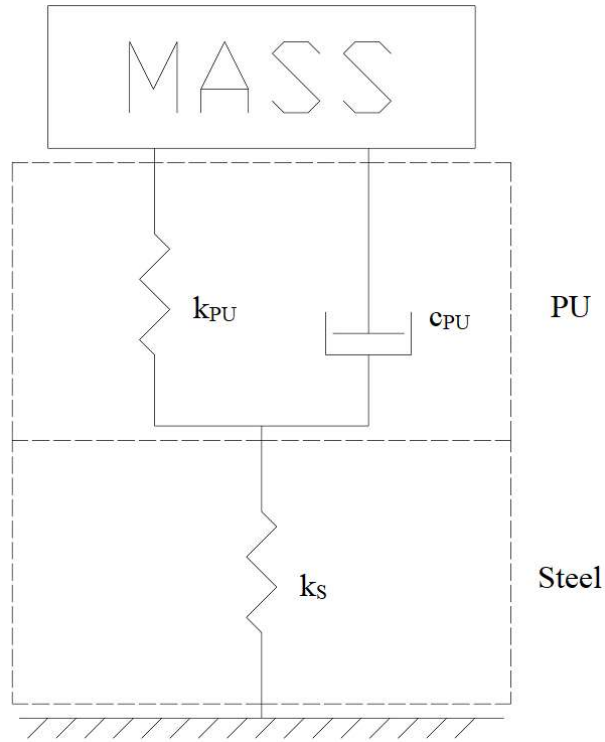


Figure 7. Analytical model of the structure.

$$\ddot{y} + \frac{k_{PU}}{c_{PU}} \dot{y} + \frac{k_{PU}}{m} y = 0 \quad (1)$$

Maxwell model under impact loading can be represented with equation 1. With initial conditions being $y(0) = 0$, $\dot{y} = v_0$ and $\ddot{y}(0) = 0$. Where, \ddot{y} = jerk, \dot{y} = acceleration, y = velocity, y = displacement, v_0 = initial speed in Maxwell model. (Meram 2019, p. 3)

In this thesis' frame the viscoelastic behavior of the polyurethane buffer and the dynamic response of the steel structure as displacement can be represented as a sum of the Maxwell model of PU and elasticity of the steel as a series with different properties representing the different materials. Meram describes in detail the solution to Maxwell model of polyurethane as maximum displacement of mass with the required definitions in his 2019 article (Meram 2019, p.3).

2.5 Scope

The scope of this thesis was set to include only one type of buffer setup with two different plate configurations. With this it is possible to find out if the implemented methods can be translated to more than one buffer configuration. These two buffer configurations were tested with different speeds. Table 1 defines the tested impact speeds for different plate configurations of the assembly.

Table 1. Tested impact speeds of different plate configurations.

Strong plate test speeds [m/s]	Weak plate test speeds [m/s]
1.00	1.00
1.75	1.75
2.50	

The 1.0 m/s speed tests were used as the reference data as the tested extension structures were originally designed according to EN 81-20 prescribing the 1.0 m/s as the maximum rated speed. All impact speeds were tested in an experimental drop test to achieve reference data. The test evaluation criteria were chosen according to EN 81-20 to be permanent deformations. Possible high stress concentrations were also inspected but these were only used to assess analysis accuracy.

3 METHODS

This chapter defines the utilized methods for evaluating the buffer structure under impact loading. Reference data for numerical methods was created with experimental testing. Utilized FE-methods are presented on a general level and their selection for this application are explained.

3.1 Drop test

An experimental drop test was performed according to EN 81-50 chapter 5.5.3. which describes in detail how to perform a buffer validation drop test. For the extent of this thesis some small exceptions were taken. Only maximum mass impacts were tested, because the intent was not to validate the buffers but to study higher than rated speed impacts. In addition to this the evaluation of test specimen focused only on the permanent deformations. Drop tests were performed to create experimental reference data that can be used to validate the other numerical methods. The drop tests were performed by dropping an elevator counterweight with the maximum rated mass of 1500 kg from controlled height to reach the desired impact speed at the point of impact to the buffer. 1500 kg is the maximum rated load for the D3 type buffer. During the tests the following output data was recorded: acceleration over time, force over time and speed over time with a load cell, a cable potentiometer, and an accelerometer. Tests were performed with identical setups for both plate configurations and specified speeds presented in Table 1.

$$v^2 = v_0^2 + 2g(x - x_0) \quad (2)$$

To reach the desired impact speeds, drop heights were calculated with equation 2 of uniformly accelerated motion in free fall by solving x , with initial conditions being $v_0 = 0$, $x_0 = 0$ and $v =$ desired impact speed. Where, $v =$ impact speed at point of time t , $g =$ acceleration due to standard earth gravity, $x =$ height of a falling object at point t and $x_0 =$ height of the falling object at starting point of time t_0 .

In Figure 8 an example of the drop test setup is presented with a guiderail supported buffer. In this thesis a standing buffer was evaluated but the test setup was identical.

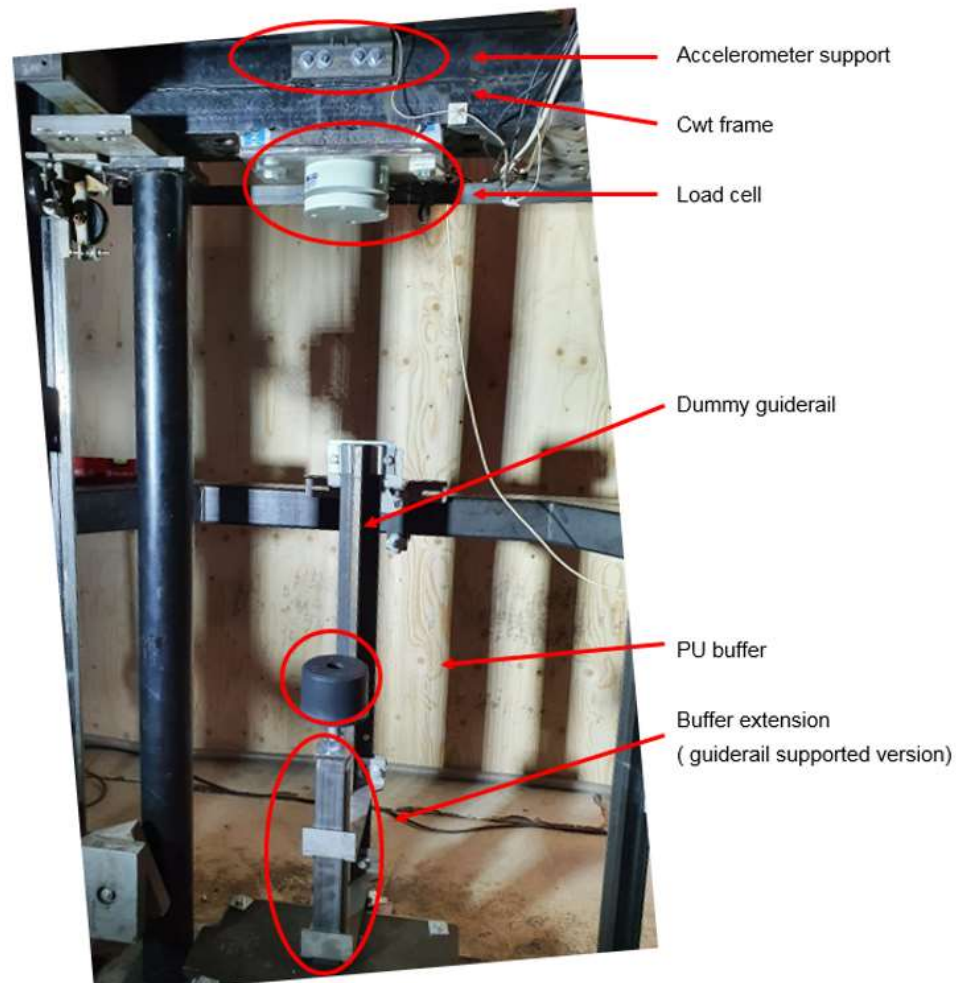


Figure 8. Drop test setup.

3.2 Static FE-analysis

Static structural finite element analysis is very widely used today in industry. It is generally the most commonly used application of finite element method in mechanical design. Structural finite element method is a numerical method to approximate stresses and strains in structures by dividing the full model to a set of simple elements. The displacements and forces applied to these elements can then be calculated to reach an equilibrium state from which the solutions to desired problem can be computed. Finite element solution accuracy is highly influenced by the element mesh and its' quality. Generally, the more elements and

how close the element shape is to the ideal shape for desired element type increases the accuracy of the analysis. This in turn will lead to longer solving times, because higher element count significantly increases the number of nodes to be solved. (Li 2021, p. 1-2.)

Static FE-analysis can be linear or nonlinear. In a linear analysis the input and the output are linear, which means that when a load is applied to the system the displacements it induces are linear. The linear static FE-analysis is based on the assumption that the loads are applied slowly enough for the system to deform linearly. This might not be true in real-life applications, but the main benefit of a linear static analysis is the easy solution, they are easier to solve than nonlinear systems. (Kim 2015, p. 81-83.) Nonlinear FE-analysis includes some type of nonlinearity in the modelled system (Kim 2015, p. 82). For the application for this thesis the nonlinearity was included in material models. The stress-strain behavior of the steel can mostly be assumed as linear material behavior, but to compute the possible plastic deformations to the steel, some plastic behavior to the material model needs to be included.

3.3 Explicit dynamic FE-analysis

One of the main focuses of this thesis was to test the implementation of a dynamic finite element analysis for the problem to find out if this rapid phenomenon needs dynamic models to capture the behavior under loading. The concrete difference of dynamic FE-analysis to static FE-analysis is that the dynamic analysis can be depending on time, which means that loads induced by velocities or accelerations can also be included to the models.

For rapid impacts explicit dynamics analysis is a suitable method to simulate velocity impact of bodies and different types of materials (Yarar, Erturk & Karabay 2021, p. 2601). Static FE-analysis methods can have convergence problems due to equilibrium states, but the explicit integration method does not have this problem as it is a step-by-step predictive solving method. In other words, explicit solving method utilizes very small timesteps, and from each of these time steps the input for the next time step are solved. (Wang, Zhang, G., Ma, Yang, Zhang, Z. & Ren 2019, p. 2)

$$\rho = \frac{m}{V} = \frac{\rho_0 V_0}{V} \quad (3)$$

$$e = \frac{1}{\rho} (\sigma_{xx}\varepsilon_{xx} + \sigma_{yy}\varepsilon_{yy} + \sigma_{zz}\varepsilon_{zz} + 2\sigma_{xy}\varepsilon_{xy} + 2\sigma_{yz}\varepsilon_{yz} + 2\sigma_{zx}\varepsilon_{zx}) \quad (4)$$

Where, ρ = density, ρ_0 = initial density, V = volume of the zone, e = energy, σ = stress in different coordinate directions and ε = strain in different coordinate directions.

The inputs the time steps require are solved based on conservation of mass, momentum and energy in Lagrange coordinates. The element mesh of the system is constantly shifting with the distortions of the bodies in the model. For all time increments the density can be solved with the initial volume of the zone V_0 and initial mass $m_0 = \rho_0 V_0$ with equation 3, and the energy conservation with equation 4. These equations are solved for all elements in the model with the input values of the previous time steps. (Ciortan, Giurgiu & Pupăză. 2014.)

4 IMPLEMENTATION OF METHODS

This chapter explains in detail how the chosen research methods were applied to in this thesis' scope. The experimental drop tests were performed in KONE Reliability Laboratory in Hyvinkää. ANSYS workbench was used for the FE-analysis. First material models for linear elastic and non-linear material behavior needed to be defined, the setup of these and the dynamic and static analysis is presented. Dynamic analysis was performed first and after that similar modeling technique was copied to static analysis.

4.1 Drop test parameters

Required heights for the drop test were calculated with the formula 2. With desired impact speed values as v and acceleration as $g = 9.80665 \text{ m/s}^2$. Below are listed the required drop heights h for different impact speeds, rounded up to closest millimeter.

1. 1m/s: $h_{1.0} = 51 \text{ mm}$
2. 1.75m/s: $h_{1.75} = 157 \text{ mm}$
3. 2.5m/s: $h_{2.5} = 319 \text{ mm}$

The actual impact speeds were checked from the data and were accepted if they were at least 80% of the desired speed. The test specimens were inspected after the test for permanent deformations.

4.2 Material models for FE-analysis

Different types of material models were needed for different analysis types. Steel material behavior was defined as non-linear for both static and dynamic analysis to be able to obtain plastic deformations after the impacts. ANSYS workbench multi-linear material model calculates the elastic region of the material behavior as linear elastic before yielding, and after ultimate strength limit is reached material behavior is treated as fully plastic. Linear-elastic material behavior of steel was based on Eurocode 3 with the following properties:

- Young's modulus $E_S = 210000 \text{ MPa}$
- Poisson's value $\nu_S = 0,3$

(EN 1993-1-1 2005, p. 28)

A multi-linear isotropic hardening model in ANSYS workbench was used to represent plastic behavior of steel, the stress-strain chart for this is from ANSYS Workbench material properties is presented in Figure 9. In addition to this a density of 7850 kg/m^3 for steel was needed in dynamic analysis. Nominal values from EN 1993-1-1 for yield strength f_y and ultimate strength f_u for S355 steel were used. Ultimate strain ε_u was calculated to meet EN 1993-1-1 requirements $\varepsilon_u > 15\varepsilon_y$, where yield strain $\varepsilon_y = f_y / E_S$.

$$f_y = 355 \text{ MPa}$$

$$f_u = 510 \text{ MPa}$$

$$\varepsilon_u = 0.025$$

(EN 1993-1-1 2005, p. 25)

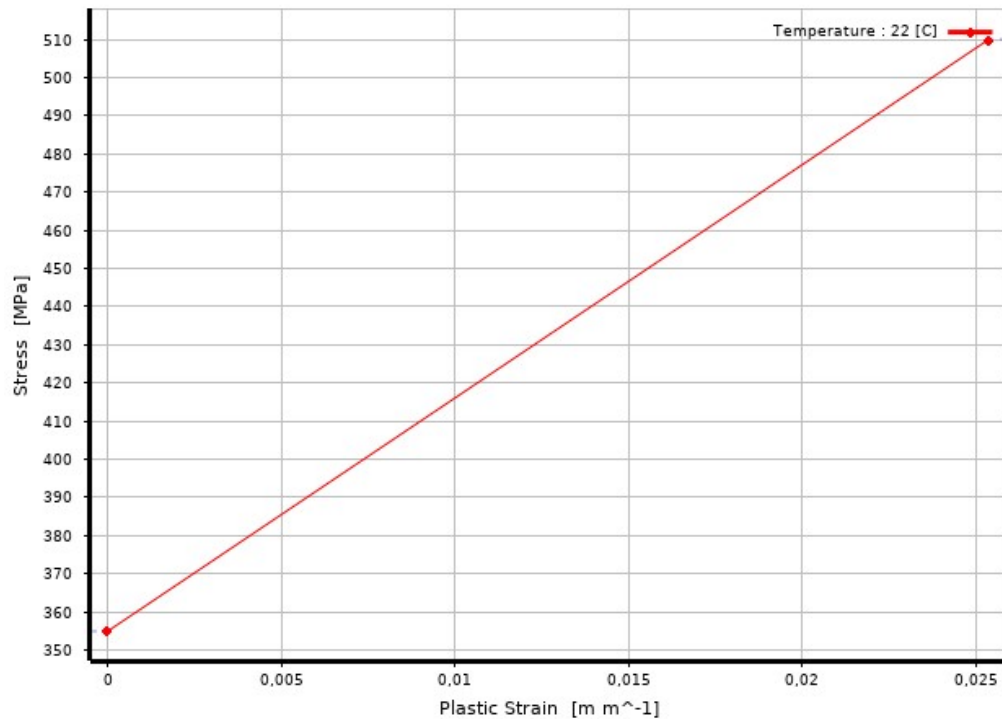


Figure 9. S355 steel multi-linear stress-strain chart in elastic-plastic regime.

PU-material behavior in static analysis was defined as nearly incompressible linear elastic material. With the following properties:

$$E_{PU} = 5 \text{ MPa}$$

$$\nu_{PU} = 0.49$$

In dynamic analysis PU material behavior was defined as nearly incompressible hyper-elastic material, with density of 550 kg/m^3 and the following constant properties of bulk modulus K and shear modulus G which are derived from the Young's modulus of the first data point of true stress-strain data presented below. ANSYS performs this conversion automatically.

$$K = 63.5 \text{ MPa}$$

$$G = 1.2785 \text{ MPa}$$

The PU-buffer material was modelled as a hyper-elastic Arruda-Boyce material model from ANSYS Workbench. ANSYS Workbench includes a curve fitting function for hyper elastic materials. Curve fitting can be done for example from biaxial stress-strain data. From the buffer manufacturer only force-deflection curves were available, so these needed first to be presented as engineering stress-strain values. Engineering stresses were calculated from initial buffer area $A = 12.272 \text{ mm}^2$ and force F . All these values are presented in Table 2.

Table 2. Engineering stress-strain values obtained from PU force-deflection.

Deflection [mm]	Longitudinal strain	Lateral strain	F [kN]	Stress [MPa] F/A
10	0.1250	0.0880	5	0.4
20	0.2500	0.1120	10	0.8
30	0.3750	0.1600	15	1.2
40	0.5000	0.2080	25	2.0
50	0.6250	0.2640	55	4.4
60	0.7500	0.3440	150	12.2
62	0.7875	0.3600	200	16.3
64	0.8000	0.4000	235	19.1

$$\varepsilon_{true} = \ln(1 + \varepsilon_{engineering}) \quad (5)$$

$$\sigma_{true} = \sigma_{engineering} \cdot (1 + \varepsilon_{engineering}) \quad (6)$$

Where, ε_{true} = true strain, $\varepsilon_{engineering}$ = engineering strain, σ_{true} = true stress and $\sigma_{engineering}$ = engineering stress. (Ling 1996, p. 38)

The obtained engineering stress-strain values needed to be converted to true stress and true strain. This can be done with equations 5 and 6. The engineering stress-strain values were converted to true stress strain values and are presented in Table 3. With these values curve fitting for hyper-elastic Arruda-Boyce model was done, with least-squares method in ANSYS Workbench. In the following Figure 10 is presented the fitted curves for non-linear hyper-elastic material behavior. ANSYS automatically calculates all necessary parameters from the curve fitting. Only incompressibility parameter needs to be defined separately and it is determined as $2/K$, where K is bulk modulus.

Table 3. True stress-strain values for PU material model.

σ_{true} [MPa]	ϵ_{true}	$\epsilon_{\text{lateral}}$
0.4500	0.118	0.088
1.0000	0.223	0.112
1.6000	0.318	0.16
3.0000	0.405	0.208
7.3125	0.485	0.264
21.3500	0.560	0.344
29.1400	0.580	0.360
34.3800	0.588	0.400

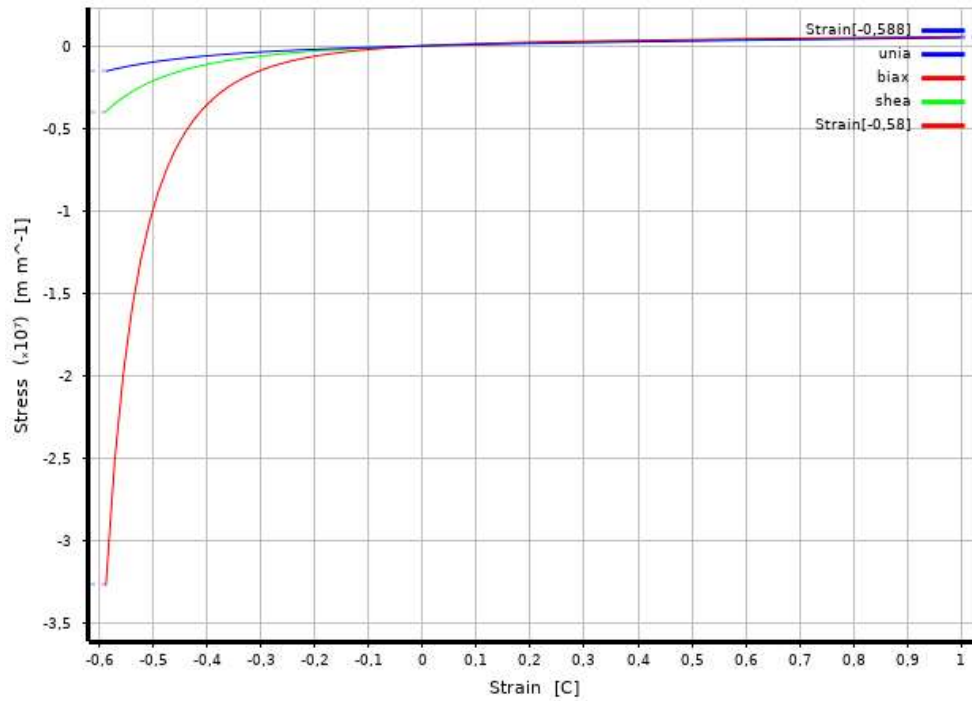


Figure 10. Hyper-elastic true stress-true strain curves for PU material behavior.

4.3 Static FE-models

The static FE-models were during the modelling process created after the dynamic models had been finalized, this was done to have equal mesh sizes for both the analysis types so that their accuracy would be comparable in terms of element sizes. Mesh was optimized for the dynamic model to induce reasonable analysis times. For the possible later applications of the results of this thesis each analysis meshes could be optimized to have more precise accuracy. In addition to this all boundary and symmetry conditions were modelled as identical to the dynamic models also. The biggest difference of the static models compared to the dynamic models is linear material properties of the polyurethane. For steel, the same multi-linear material model was used with both analysis types. Stepped loading was used to achieve unloading and from that the plastic deformations could be captured.

First, geometry import and needed simplifications to the geometry were made. The buffer was modelled as $\frac{1}{4}$ -symmetric model utilizing symmetry constraints. The buffer plates and the PU-buffer were modeled without the holes. This was done to achieve a better mesh for the plates and because $\frac{1}{4}$ -symmetry was utilized for the geometry the deformation of elements of the PU-buffer geometry in internal direction cannot be detected by the symmetry

regions and distortions will collide in internal directions. The symmetry constraints can be only applied to element sides in the initial condition. In addition to this the hole in the adjustment rod was filled to achieve more uniform mesh, the screw between PU, plate and the adjustment rod was replaced with a joint to keep the plate attached to the rod, a fully bonded contact between these surfaces would have created an unnecessarily stiff condition for the bending of the plate. Also, the threads for the rod, nut and beam top plate were removed to simplify the model.

Solid elements were used to mesh the bodies with 5 mm size elements in the buffer plates and in the PU-buffer 10 mm tetra-elements were used. For other bodies in the system a very coarse mesh was used with hex-elements if possible. This was due to the dynamic explicit solver time stepping. The solver determines the time step increments based on the smallest characteristic length element, so very small elements and overall number of elements increase the analysis solving time exponentially. The $\frac{1}{4}$ -geometry and element mesh are presented in Figure 11, symmetry regions in x and z-direction were created for the corresponding cross sections.

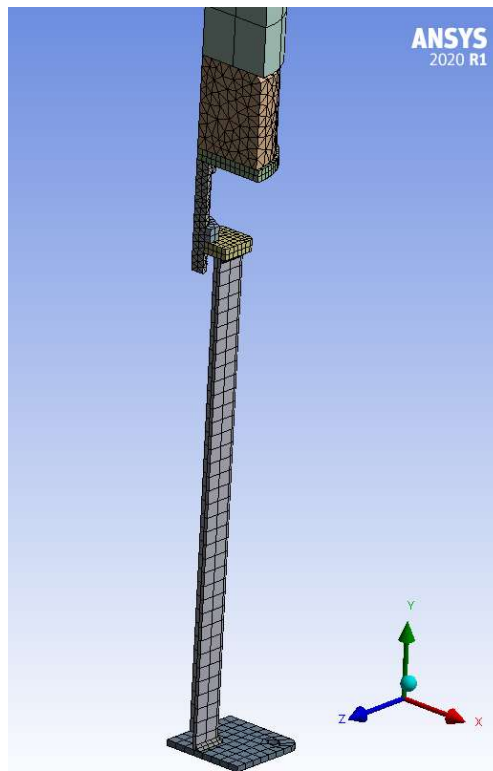


Figure 11. FE-model modelled with $\frac{1}{4}$ -symmetry.

Welded joints were modelled with no penetration. Frictional contacts between steel and steel in weak plate configuration were modelled with a friction coefficient of 0.74 as defined by Engineering Library and Hyper Textbook which have based their values on separate design manuals (Engineering library 2022, Hyper textbook 2022). PU contact with the plate and the mass were also defined as frictional contacts, and body interaction control was set as frictional contact for the possible trajectory contacts from the PU deformations reacting as frictional. Cruz Gomez et al. define in their 2013 article the frictional coefficient of rubber-steel contacts to be 0.6-1.1 (Cruz Gomez 2013, p. 1424). A conservative value of 0.8 was used for these models.

The load to the model was applied to a same size cylindrical rigid block as in the dynamic model by a distributed load on a surface. Three different types of loads were tested for the static models.

1. Load calculated with impact factor for 1.0 m/s speed impact
2. Maximum singular load value from testing data
3. Highest average load over 40 ms time interval in the impact from testing data load values

These load cases were analyzed with all impact speeds except for the impact factor load case which could only be calculated with 1.0 m/s speed due to the impact factor being defined only for 1.0 m/s impacts.

$$F = igm \quad (7)$$

The impact factor load F is calculated with equation 7 as mass times acceleration load increased by the impact factor i which for energy accumulation type buffers is $i = 3$ (EN 81-20 2020, p. 93). This assumption is based on the same standard utilizing impact factors in load calculation for example in guide rail reaction forces (EN 81-20 2020, p. 91). The maximum loading was taken as the absolute maximum load from the drop test data. Average impact loading was derived from EN 81-20 and EN 81-50 from the retardation conditions which are defined as maximum impact under 40 ms (EN 81-20 2020, p 95, EN 81-50 2020, p. 25). This can be thought of as the peak loading during the impact.

Because 1/4-symmetry is used in the models also 1/4-loads are used. The loads are set in the static analysis with stepped control to capture unloading of the structure and the plastic deformations after that. The model was fully constrained from the bottom plate.

4.4 Dynamic FE-models

Dynamic FE-models were in the process created first because the aim was to use equal element sizes for both the dynamic and the static analysis. Dynamic models are more demanding to analyze so the finalized mesh was copied to the static analysis after the dynamic models were complete. ANSYS explicit dynamics module was used to analyze the models.

The impact loading in the analysis was set as a body with mass impacting the buffer. Impact body was modelled as 1/4 of a cylindrical block with 1/4 mass (375 kg) of the full counterweight mass (1500 kg) with diameter of 130 mm, size of the block was same as in static analysis equal to the load cell size. Rigid body motion was enabled for this body and initial velocity was given in analysis settings. The model was made to represent the exact moment when the mass impacts the buffer to save analysis time, with this initial velocity could be given directly as the desired impact speed. In addition to this standard earth gravity g , could be introduced to model which applies to all bodies. The geometry was full constrained from the bottom plate as in the static analysis.

Table 4 presents the most important settings which have influence on the functionality and accuracy of the explicit analysis. These settings were used for all models by only varying the end time and the time step safety factor if needed. The end time doesn't need to be as long with the higher speed impacts and the time step safety factor changes the initial time step, it can help with solver errors in the models with higher impact speeds.

Table 4. Analysis settings for explicit dynamic analysis.

End time	0.125 – 1.5 s
Maximum Number of cycles	1×10^7
Maximum energy error	1×10^7
Minimum time step	1×10^{-30} s
Time step safety factor	0.45 – 0.9
Hourglass damping	Flangan Belytschko
Stiffness Coefficient	0.03
Result number of points	$\sim 2500/0.05$ s

Two different types of loading cases were analyzed with the impact speeds v presented in Table 1.

- Load case 1: Initial velocity v
- Load case 2: Initial velocity v and standard earth gravity g

Unloading for the dynamic models was done by first finding the point in the impact after which the velocity of the impacting body has reached 0. In load stepping the acceleration was then after this point in the simulation changed to negative direction, which means that after this the impacting body will start traveling upward. This was found to be the most stable way of creating the unloading for the dynamic models. It is not possible to do stepped unloading as in static models, because in dynamic loading the accelerations are tied to all bodies of the model and cannot be turned off.

5 RESULTS

This chapter presents the results of all research methods. The results mainly focus on the deformation of the buffer plates, these are parts of the buffer assembly which have clearly visible deformations. Other critical spots are also presented in this thesis, but the main result evaluation is focused on the deformation of the buffer plates. The results first present the experimental drop test results because they are needed to define loads for the static analysis, after which the results from the FE-analyses are presented.

5.1 Drop test results

Drop test results were assessed from the buffer plates by measuring the deformation from the impact. The deformation was measured from the edge of the plates by placing the plates on a flat surface upside down and finding the highest point of the edge with a vernier caliper and subtracting the plate thickness T from the obtained value. Example of this measurement is presented in Figure 12.

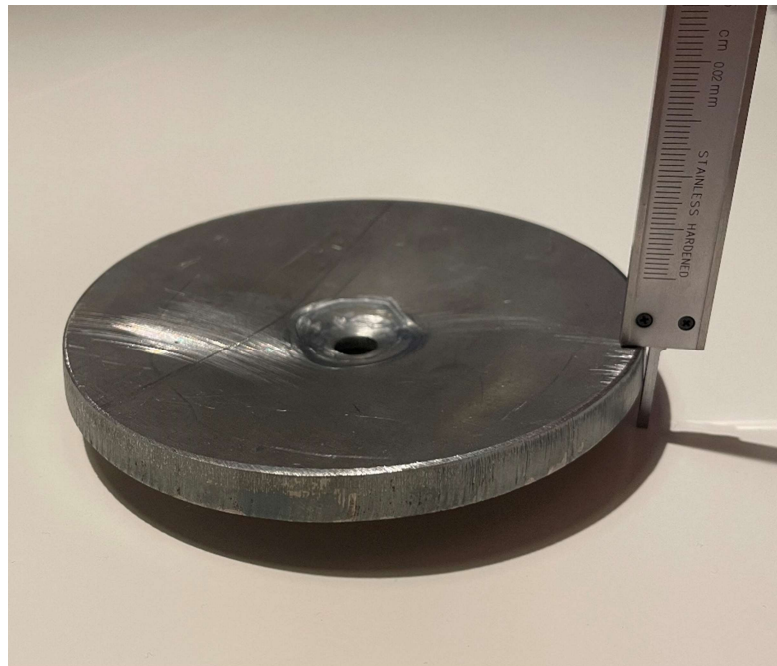


Figure 12. Measurement of plate deformations in drop tests.

The weak plates had some initial deformation originating from welding heat input. An example of this is presented in Figure 13. The measurement of this was done as described previously. Initial deformation in the weak plates was measured to be approximately 1.1 mm. The initial deformations were subtracted from the weak plate total deformation values.

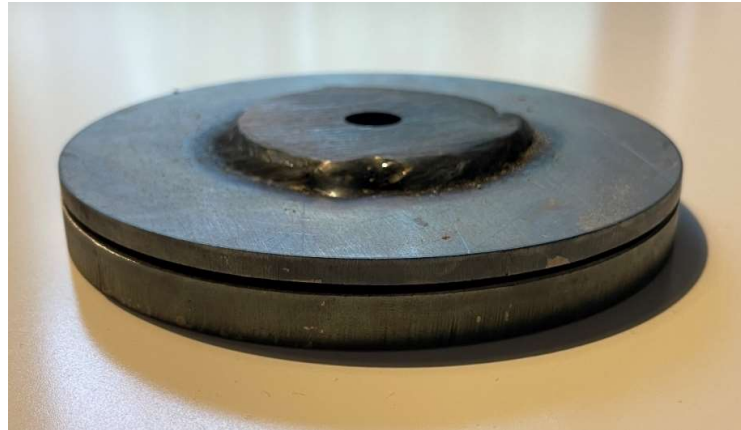


Figure 13. Initial deformation in the weak plate.

In Table 5 is presented the total deformations of the plates in drop tests. In weak plate values the initial deformation has been subtracted from the absolute values. Necessary values from drop test data for static load definitions were logged by a load cell with 25 Hz measuring frequency.

Table 5. Plastic deformation results in drop tests.

Structure configuration and impact speed	Plastic deformation [mm]
Strong plate $v = 1.0$ m/s	0.00
Weak plate $v = 1.0$ m/s	0.00
Strong plate $v = 1.75$ m/s	0.50
Weak plate $v = 1.75$ m/s	3.20
Strong plate $v = 2.5$ m/s	9.82

In Table 6 is presented the force values from drop tests necessary for static analysis. Maximum forces are absolute maximum recorded values and average values are the highest average of all force values in 40 ms range. These were used to create static analysis load cases.

Table 6. Impact force values from drop-test data.

Structure configuration and impact speed	Maximum load [N]	Average load over 40 ms interval [N]
Strong plate $v = 1.0$ m/s	52283	46248
Weak plate $v = 1.0$ m/s	61585	51765
Strong plate $v = 1.75$ m/s	124087	86445
Weak plate $v = 1.75$ m/s	122108	87583
Strong plate $v = 2.5$ m/s	201642	123680

5.2 Static FE-analysis results

The force for static model of impact value loading case was calculated with equation 7 to be 44145 N and divided by 4 because of the $\frac{1}{4}$ -symmetry. The values for maximum and average loading cases for static analysis were recorded from the experimental drop test load cell and divided by 4. The force values used in the static analysis are presented in Table 7.

Table 7. Loading cases for static analysis.

Structure configuration and impact speed	Impact factor load [N]	Maximum load [N]	Average load over 40 ms interval [N]
Strong plate $v = 1.0$ m/s	11036	13071	11562
Weak plate $v = 1.0$ m/s	11036	15396	12941
Strong plate $v = 1.75$ m/s	-	31022	21611
Weak plate $v = 1.75$ m/s	-	30527	21896
Strong plate $v = 2.5$ m/s	-	50411	30920

Results for deformations were recorded from the FE-models as closely the same way as to the experimental test specimen as possible. The deformation of the plate bottom edge, plate top center point and the face on top of the rod were plotted in y-direction with deformation probes in analysis post processing. The deformation probes plot the total deformation of the selected points inside the coordinate system in the selected direction. The edge and the center point are needed for calculating the total deformation in the plate. The values from top of the rod are subtracted from the plate deformation to remove the possible deformations in the lower part of the structure to achieve the most accurate result for the total deformation of the plate only. There is no possibility in ANSYS to record a geometry specific value of a body, only the total deformation inside the coordinate system is available. The placement of deformation probes on the geometry are presented in Figure 14, with these it is possible to achieve the closest comparison to experimental measurements.

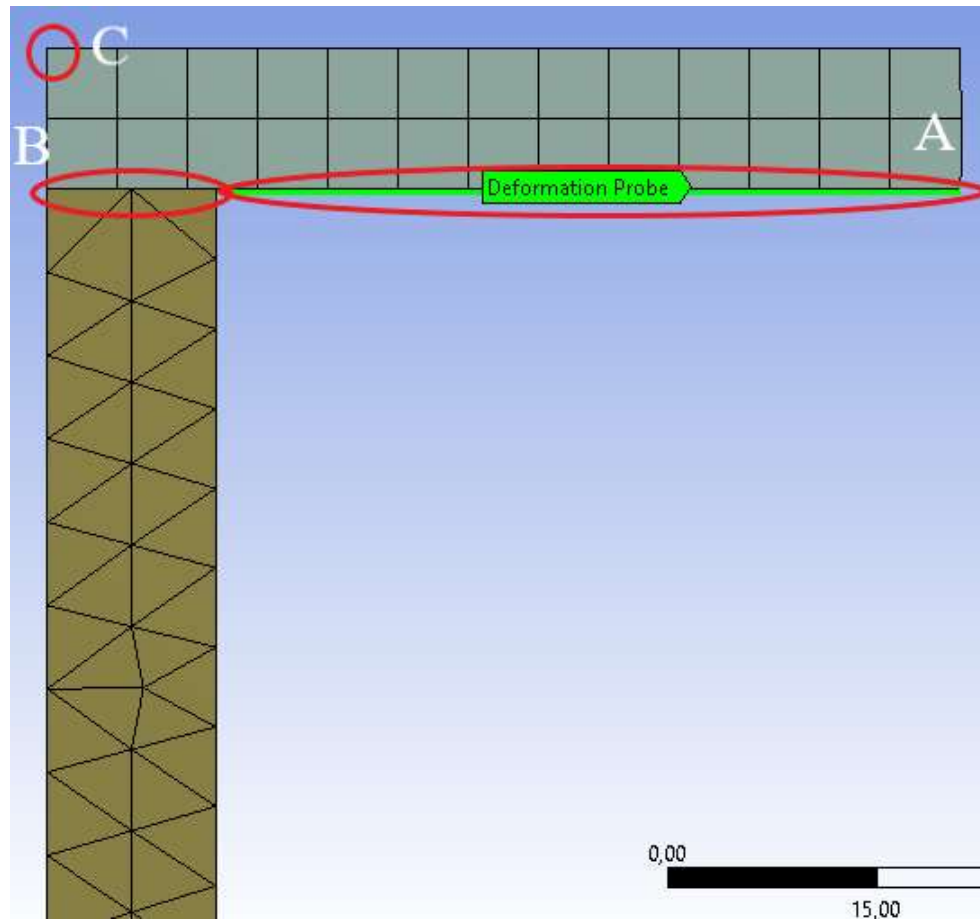


Figure 14. Deformation probes for FE-models. A = Plate bottom edge, B = Rod top surface and C = Plate top center.

The total deformation of the plates in the models can be calculated as follows: $(A-B)-(C-B)$. The values were recorded after unloading to capture the plastic deformation. These values are presented in the following Table 8 and the calculated total deformations of are presented in Table 9 as absolute values. The equivalent von Mises stress distributions for the models are presented in Figures 15, 16, 17, 18 and 19.

Table 8. Static analysis deformation values [mm].

Structure configuration and impact speed	Deformation values [mm] Impact factor load	Deformation values [mm] Maximum load	Deformation values [mm] Average load
Strong plate $v = 1.0$ m/s	A = -0,000071692 B = 0,000093095 C = 0,000096808	A = -0,000413710 B = 0,000283380 C = 0,000296920	A = -0,000104930 B = 0,000133550 C = 0,000138920
Weak plate $v = 1.0$ m/s	A = -0,007799900 B = 0,000195390 C = 0,000265510	A = -0,130570000 B = 0,001877900 C = 0,002618900	A = -0,029160000 B = 0,000605100 C = 0,000840500
Strong plate $v = 1.75$ m/s	-	A = -0,902050000 B = 0,011778000 C = 0,022335000	A = -0,101240000 B = 0,004953000 C = 0,011260000
Weak plate $v = 1.75$ m/s	-	A = -24,792000000 B = 0,044227000 C = 0,056974000	A = -2,101200000 B = 0,011943000 C = 0,016809000
Strong plate $v = 2.5$ m/s	-	A = -28,911000000 B = -0,712250000 C = -0,769230000	A = -0,887240000 B = 0,011632000 C = 0,013972000

Table 9. Total deformations of the plate in static analysis.

Structure configuration and impact speed	Deformation [mm] Impact factor load	Deformation [mm] Maximum load	Deformation [mm] Average load
Strong plate $v = 1.0$ m/s	0,000169	0,000711	0,000244
Weak plate $v = 1.0$ m/s	0,000807	0,133189	0,030001
Strong plate $v = 1.75$ m/s	-	0,924385	0,112500
Weak plate $v = 1.75$ m/s	-	24,848970	2,118009
Strong plate $v = 2.5$ m/s	-	28,141770	0,901212

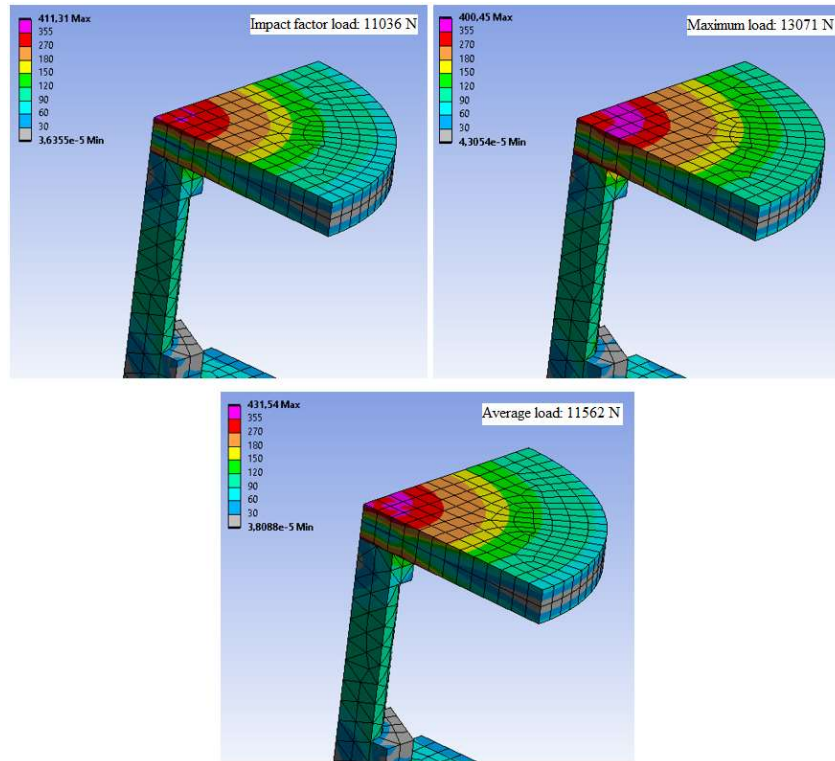


Figure 15. Static results for strong plate 1.0 m/s impact, equivalent von Mises stress [MPa].

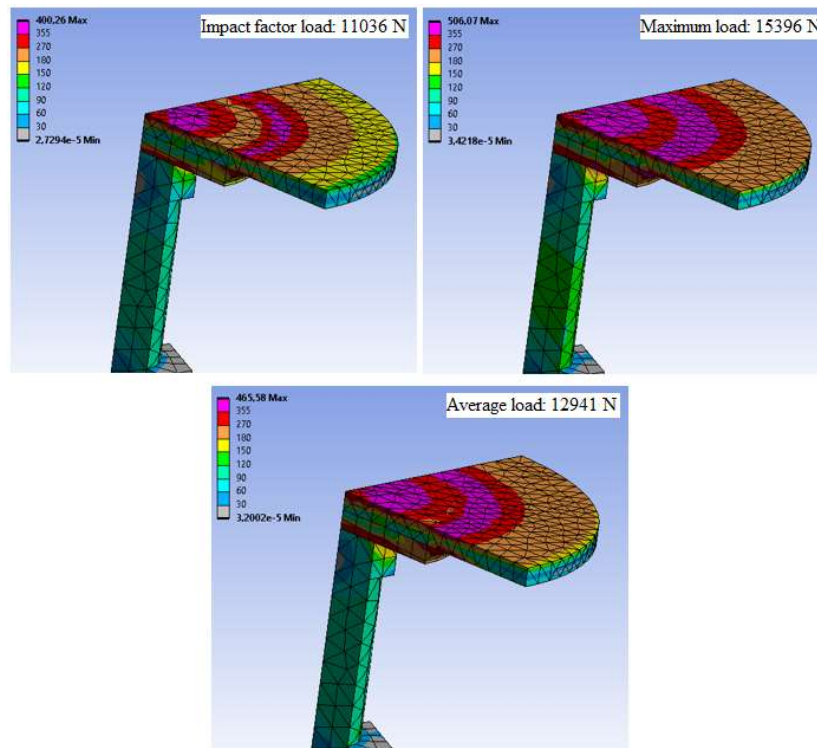


Figure 16. Static results for weak plate 1.0 m/s impact, equivalent von Mises stress [MPa].

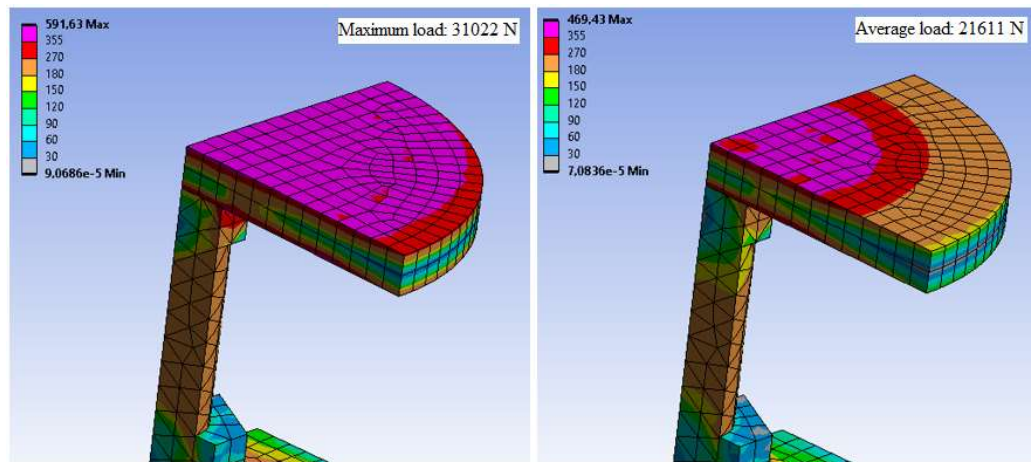


Figure 17. Static results for strong plate 1.75 m/s impact, equivalent von Mises stress [MPa].

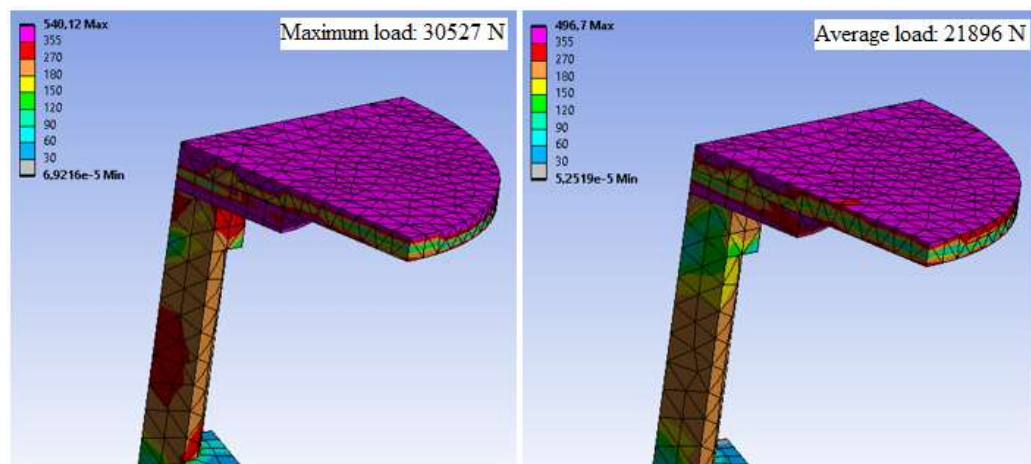


Figure 18. Static results for weak plate 1.75 m/s impact, equivalent von Mises stress [MPa].

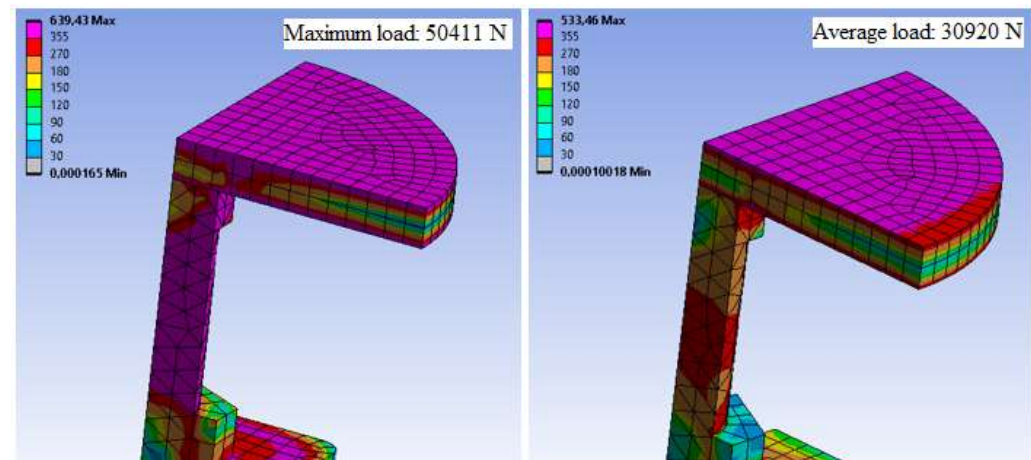


Figure 19. Static results for strong plate 2.5 m/s impact, equivalent von Mises stress [MPa].

5.3 Dynamic FE-analysis results

The results for plate deformation for dynamic analysis were taken from the same points in the model as they were for the static analysis and the total deformation was also calculated the same way. The difference in recording the results is that for dynamic analysis that these are recorded from the model after unloading as average values, after the deformation has set to a constant value. The average is needed because there is some vibrance in the system so the values are varying a bit after the unloading but this is only in fractions of millimeter so a good approximation can be made with an average. In Figure 20 is presented an example of how the deformation plots look like in ANSYS Workbench. For example, for this the result the average would be calculated from the result points between 0.125 s and 0.15 s.

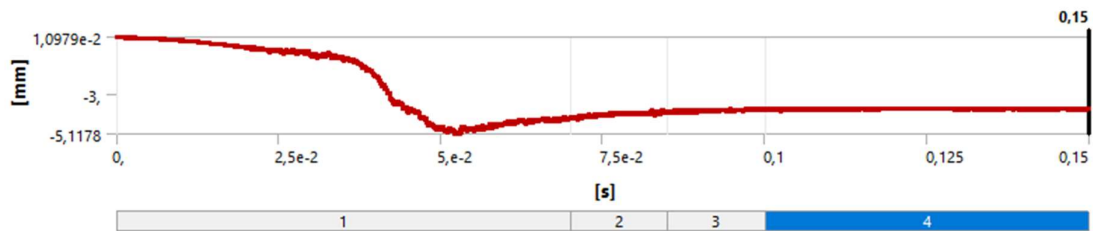


Figure 20. Example of deformation probe graph from dynamic analysis.

In the following Table 10 is presented the approximated deformation values from the dynamic analysis's, from which all the total deformations were calculated. The total calculated deformations are presented in Table 11 as absolute values. The equivalent von Mises stress distributions for the models are presented in Figures 21, 22, 23, 24 and 25. The stress distributions were taken from the point of largest deformation during the simulation.

Table 10. Dynamic analysis deformation values.

Structure configuration and impact speed	Deformation values [mm]	
	Load: v	Load: $v + g$
Strong plate $v = 1.0$ m/s	A = -0,660166451 B = -0,658679910 C = -0,654070980	A = -0,691681447 B = -0,690489380 C = -0,671176580
Weak plate $v = 1.0$ m/s	A = -0,741297802 B = -0,673199620 C = -0,673199620	A = -1,183482414 B = -0,544670400 C = -0,544670400
Strong plate $v = 1.75$ m/s	A = -0,908830000 B = -0,873380000 C = -0,845580000	A = -3,807930000 B = -1,686270000 C = -1,664980000
Weak plate $v = 1.75$ m/s	A = -2,225210000 B = -0,641790000 C = -0,641790000	A = -8,569380000 B = -2,433230000 C = -2,433230000
Strong plate $v = 2.5$ m/s	A = -9,154310000 B = -3,835210000 C = -3,893520000	A = -15,258900000 B = -7,949780000 C = -8,015180000

Table 11. Total deformations of the plate in dynamic analysis.

Structure configuration and impact speed	Deformation [mm]	
	Load: v	Load: $v + g$
Strong plate $v = 1.0$ m/s	0.006095	0.020505
Weak plate $v = 1.0$ m/s	0.068100	0.638810
Strong plate $v = 1.75$ m/s	0.063240	2.142940
Weak plate $v = 1.75$ m/s	1.583420	6.136150
Strong plate $v = 2.5$ m/s	5.260800	7.243670

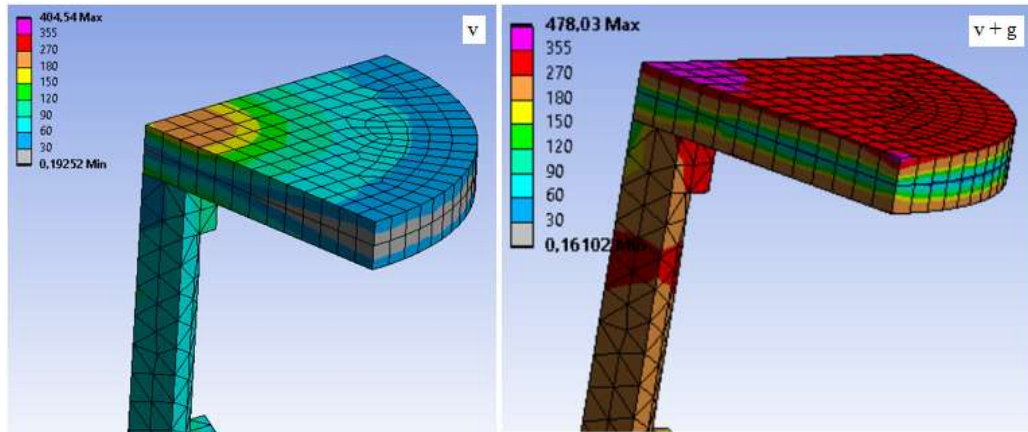


Figure 21. Dynamic results for strong plate 1.0 m/s impact, equivalent von Mises stress [MPa].

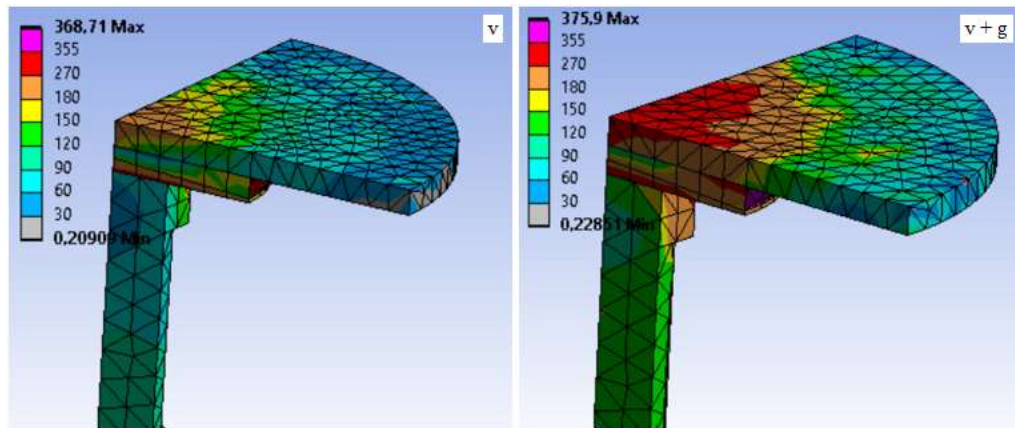


Figure 22. Dynamic results for weak plate 1.0 m/s impact, equivalent von Mises stress [MPa].

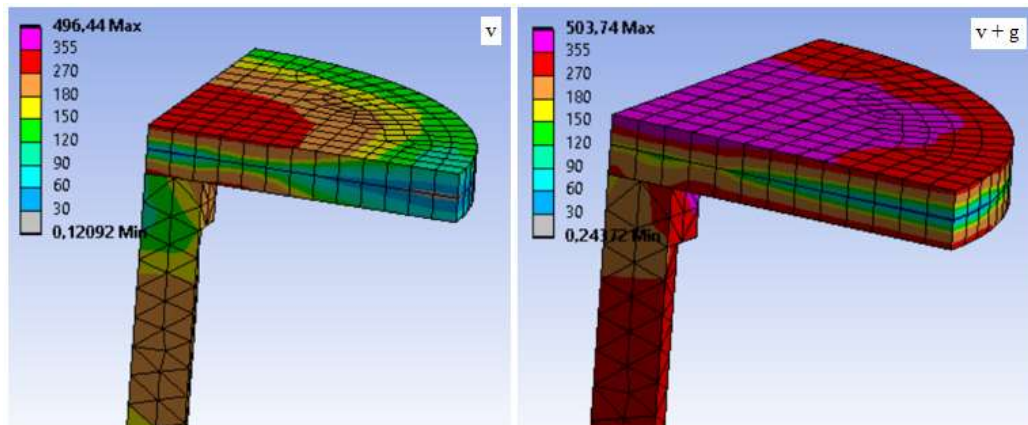


Figure 23. Dynamic results for strong plate 1.75 m/s impact, equivalent von Mises stress [MPa].

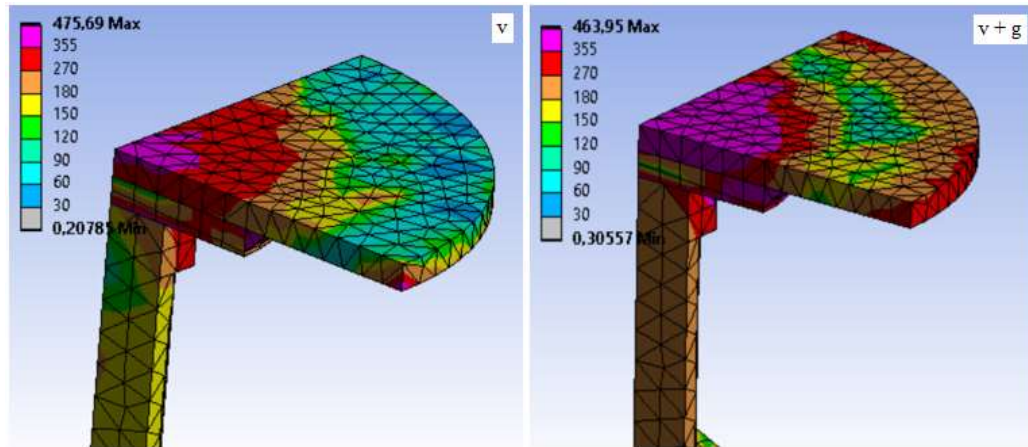


Figure 24. Dynamic results for weak plate 1.75 m/s impact, equivalent von Mises stress [MPa].

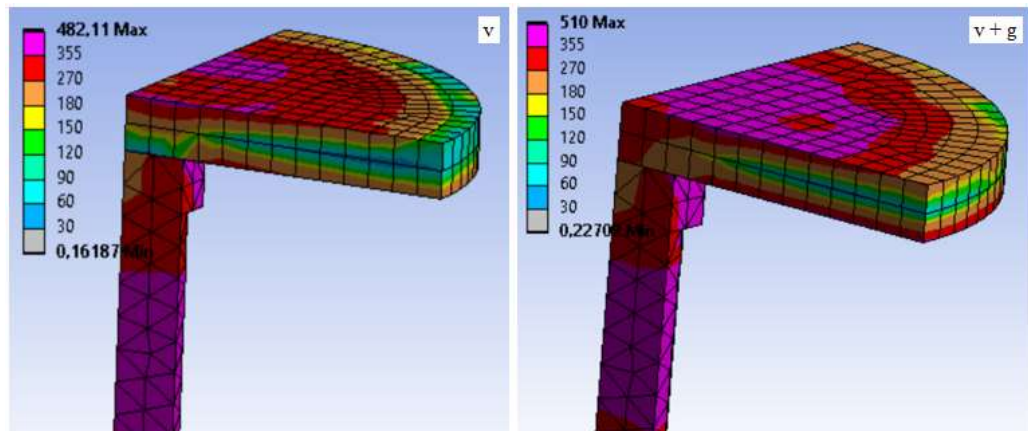


Figure 25. Dynamic results for strong plate 2.5 m/s impact, equivalent von Mises stress [MPa].

In Figures 26, 27, 28, 29 and 30 are presented the speeds during the impacts in dynamic analysis with different loadings including the speed of the impact in experimental results as the reference. It is important to note that in the experimental results the update interval of the accelerometer is much larger than the interval of the datapoints in the analysis.

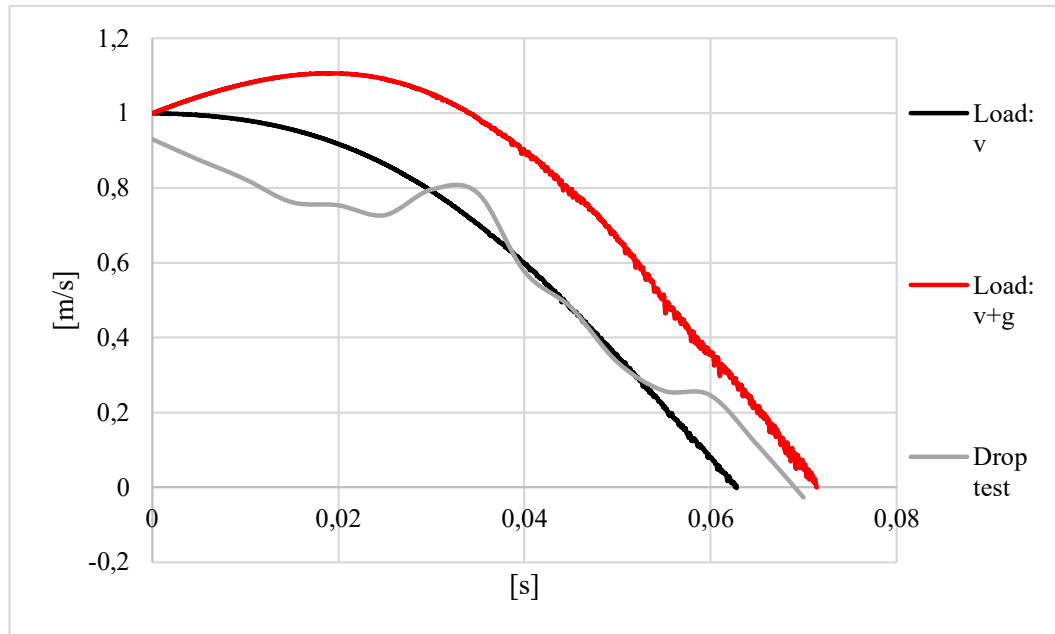


Figure 26. Speed of the impacting mass during 1.0 m/s impact in dynamic analysis and drop test in strong plate configuration.

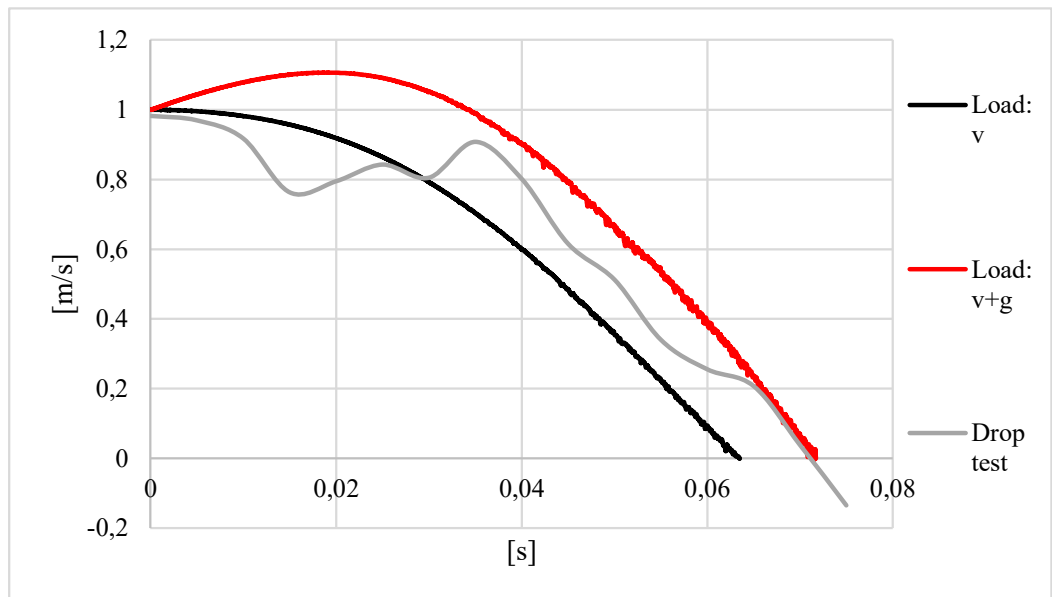


Figure 27. Speed of the impacting mass during 1.0 m/s impact in dynamic analysis and drop test in weak plate configuration.

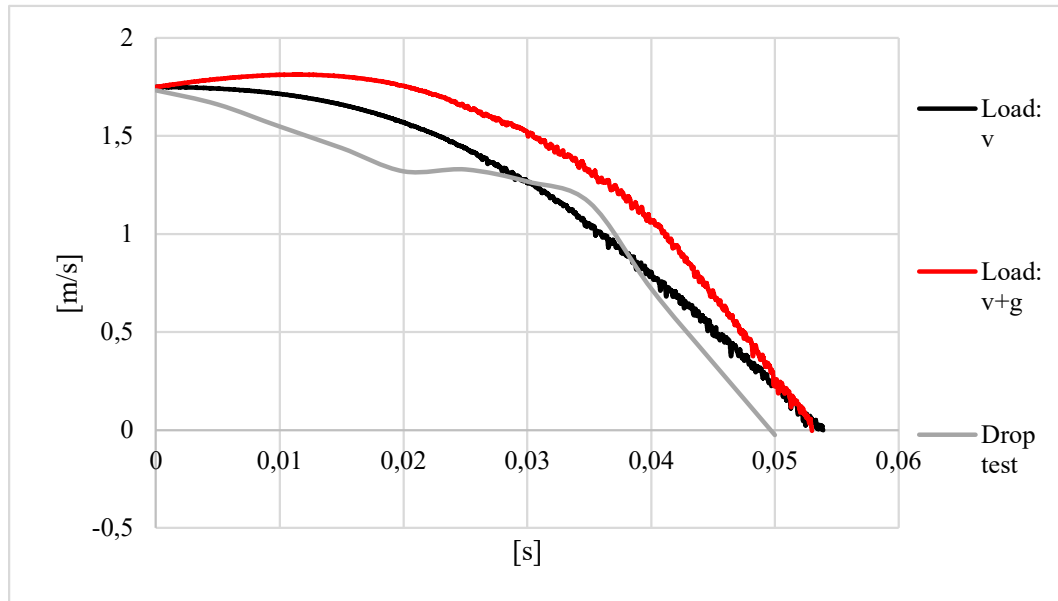


Figure 28. Speed of the impacting mass during 1.75 m/s impact in dynamic analysis and drop test in strong plate configuration.

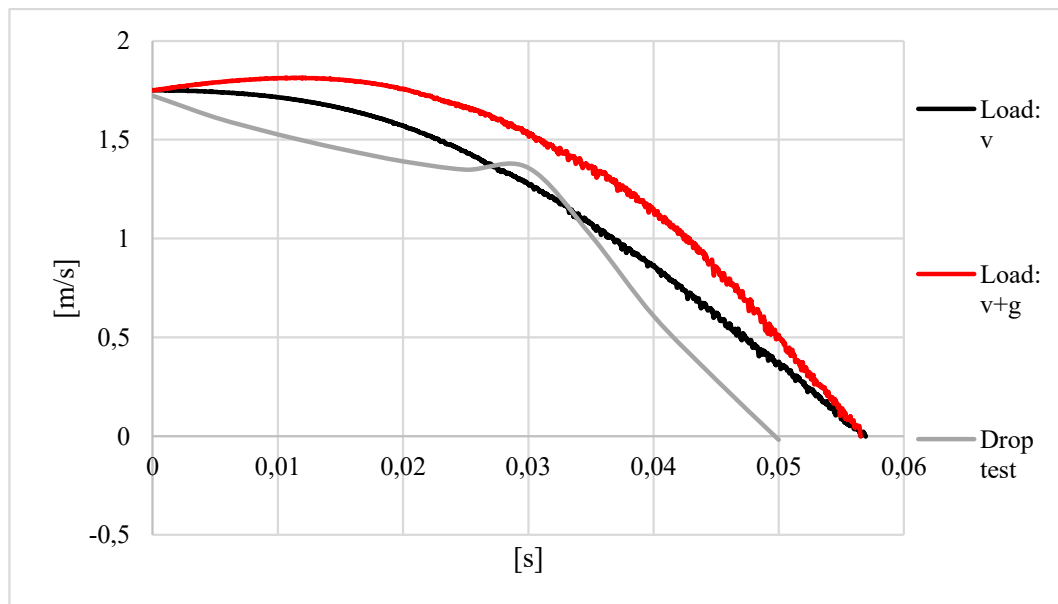


Figure 29. Speed of the impacting mass during 1.75 m/s impact in dynamic analysis and drop test in weak plate configuration.

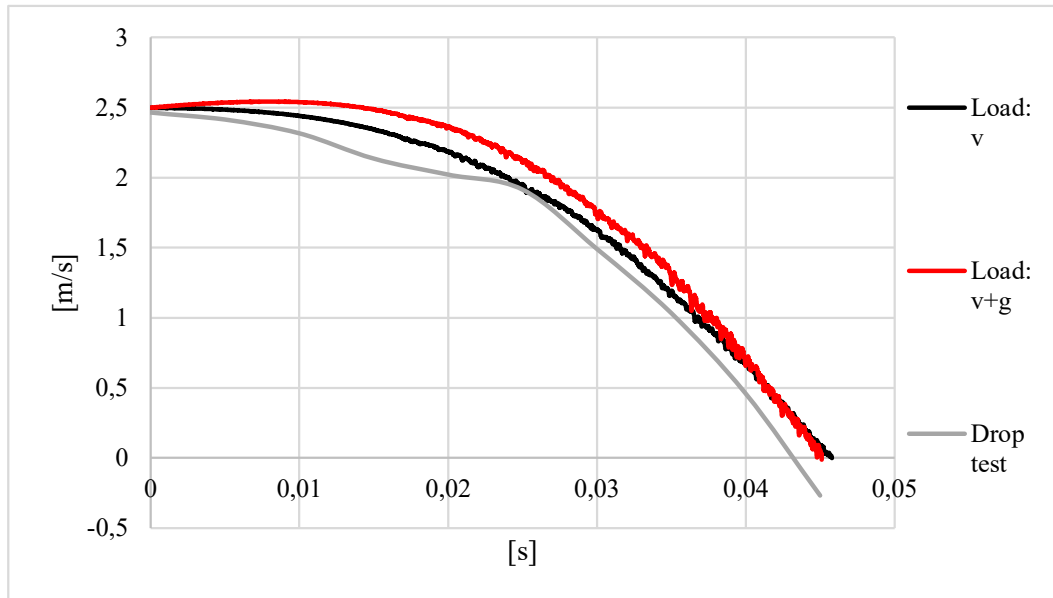


Figure 30. Speed of the impacting mass during 2.5 m/s impact in dynamic analysis and drop test in strong plate configuration.

6 ANALYSIS & DISCUSSION

This chapter presents the most important findings from the results by analyzing the deformation results compared to each other. From these findings the best methods for design purposes are proposed. In addition to this by analyzing reliability, sensitivity, and validity of the methods suggestions for further improvements are made.

6.1 Result comparison

In the following Figures 31, 32, 33, 34 and 35 are presented the plate deformations for all analyzed impact speeds with all the different loading and analysis cases. The experimental drop test results act as the baseline to which the different types of analysis results are compared to. The bar diagrams can be thought of as visual representations of the deformations.

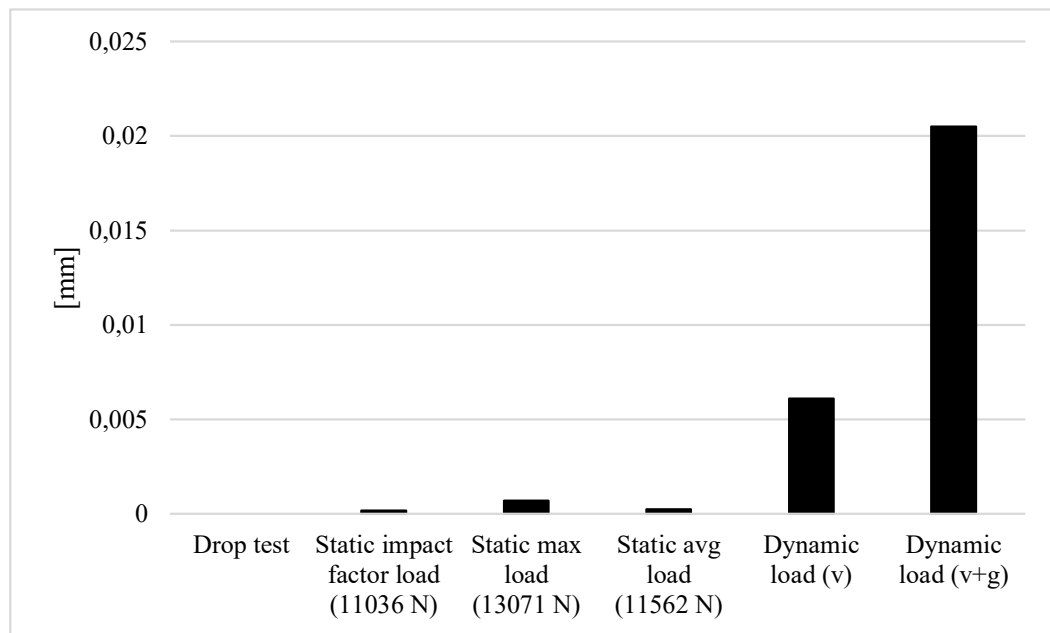


Figure 31. Strong plate 1.0 m/s deformation result comparison.

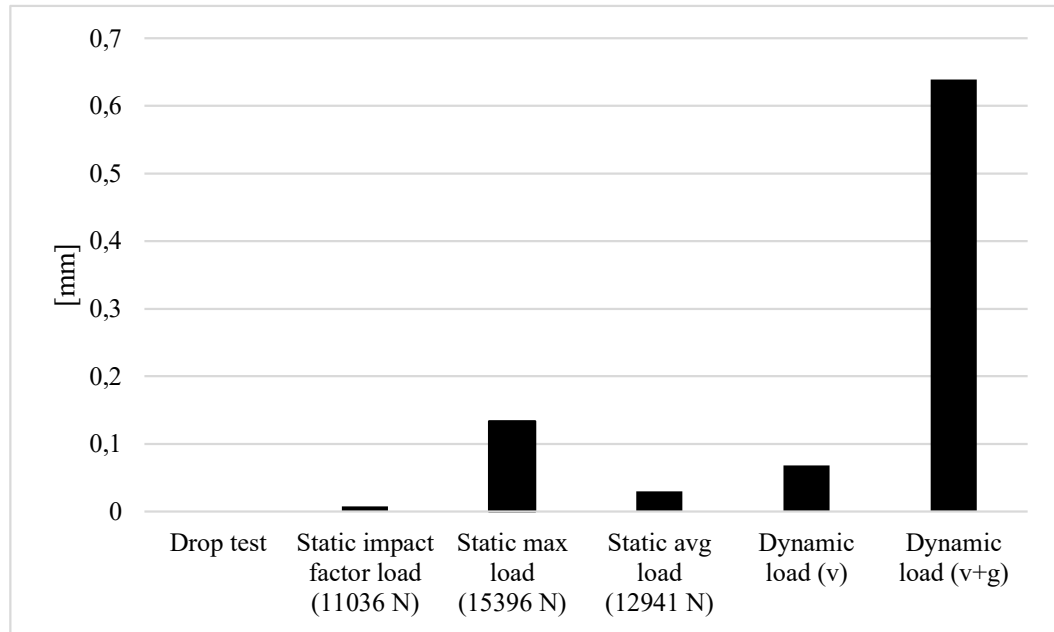


Figure 32. Weak plate 1.0 m/s deformation result comparison.

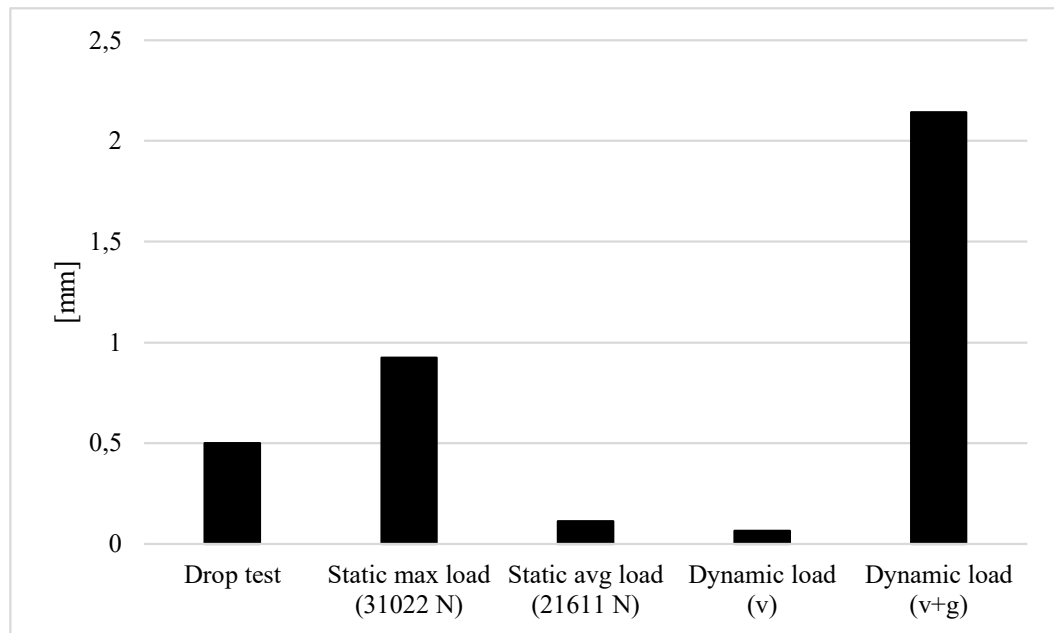


Figure 33. Strong plate 1.75 m/s deformation result comparison.

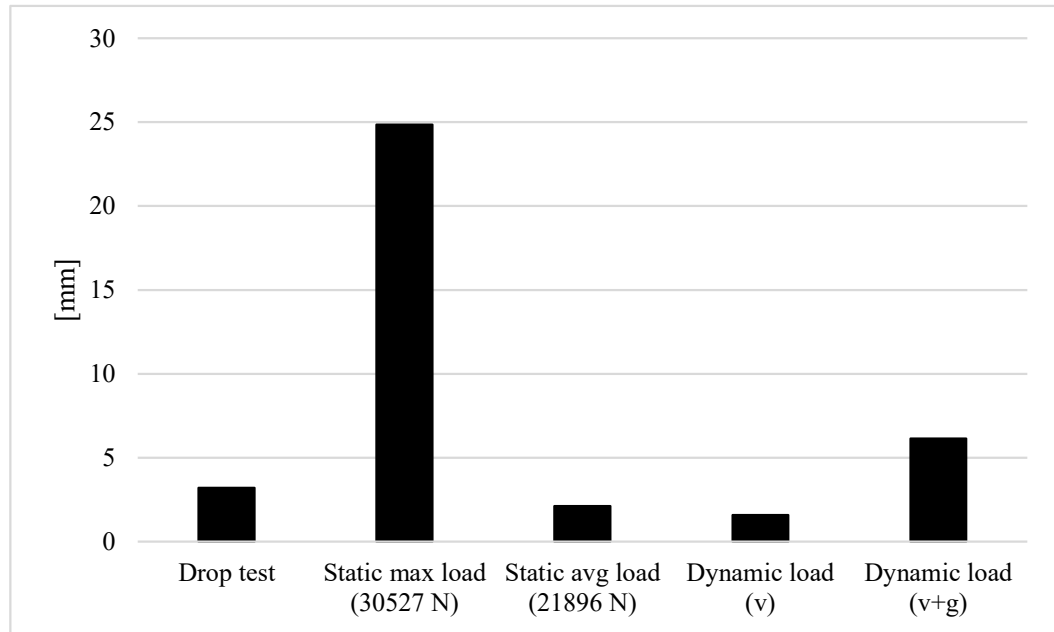


Figure 34. Weak plate 1.75 m/s deformation result comparison.

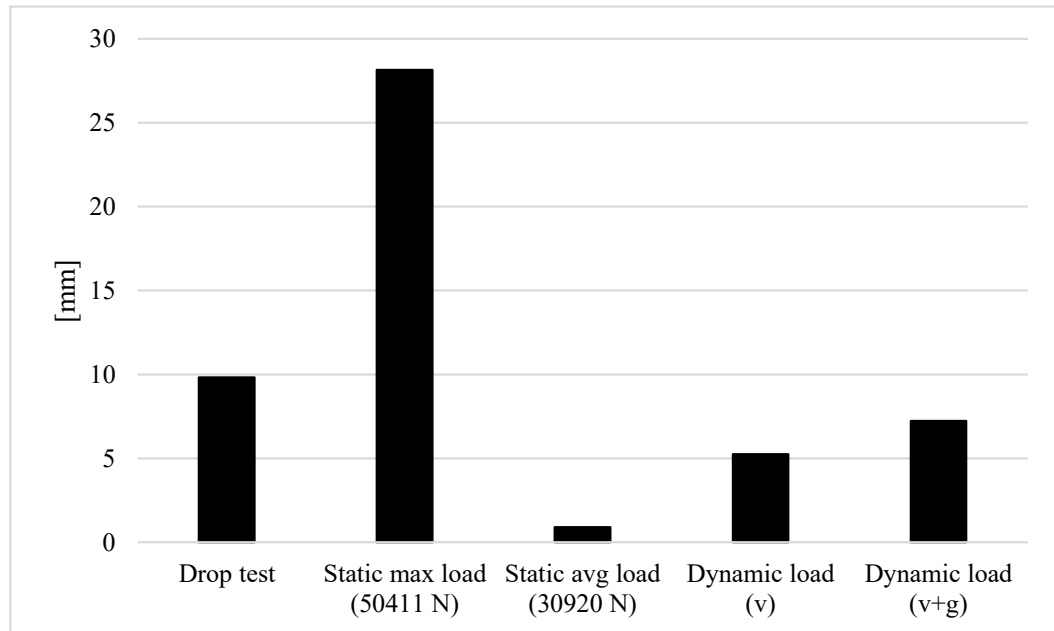


Figure 35. Strong plate 2.5 m/s deformation result comparison.

In Table 12 is presented the difference of the result magnitudes from all analysis' compared to the drop test results. A negative value signifies that the result is smaller compared to the drop test result and a positive value signifies that the result is larger.

Table 12. Magnitude differences in analysis versus experimental test.

Structure configuration and impact speed:	Static impact factor load	Static maximum load	Static average load	Dynamic load v_0	Dynamic load $v_0 + g$
Difference [mm] Strong plate $v = 1.0$ m/s	0,000169	0,000711	0,000244	0,006095	0,020500
Difference [mm] Weak plate $v = 1.0$ m/s	0,008065	0,133189	0,030001	0,068098	0,638812
Difference [mm] Strong plate $v = 1.75$ m/s		0,424385	-0,387500	-0,436760	1,642943
Difference [mm] Weak plate $v = 1.75$ m/s		21,648970	-1,081990	-1,616580	2,936149
Difference [mm] Strong plate $v = 2.5$ m/s		18,321770	-8,918790	-4,559200	-2,576330

From these previous figures and the magnitude table, a couple of clear observations can be made. Firstly, regarding the first research question of the validity of the impact factor loading can be verified. The impact factor loading provides in both the strong plate and the weak plate configurations plastic deformation results of approximately 0.0002 mm and 0.008 mm respectively, which are very close to the experimental drop test result of no-deformation. The other methods for 1.0 m/s impacts also provide acceptable results for determining the no-deformation condition with very small total deformation results but the impact factor loading is the closest to 0 mm deformation. Secondly, when inspecting the higher impact speed results, it is clear that using the absolute maximum load value from drop-tests as the load case is too much to be used for the static analysis. The static maximum load cases are in all high-speed impacts yielding too large deformation results. Thirdly, it is very clear that for the dynamic analysis with only the initial impact speed for the loading is not enough to induce adequate load to the system to yield proper deformation results. That is to say, standard earth gravity is necessary in the dynamic models.

Other observations can also be made when cross examining similar load cases for different plate configurations. For example, when first looking at the strong plate 1.75 m/s results it seems like that static maximum load would yield the closest results compared to the drop-tests but for the 2.5 m/s impact the static maximum load is very clearly too much. The same is also true for the weak plate 1.75 m/s model. The maximum load from the strong plate 1.75 m/s drop test seems to just coincidentally correspond to create results closest to the experimental data. Maximum loading is also very problematic in the weak plate configuration. Some of this is probably consequence from the frictional contact between the plates. In static analysis the frictional contact will slip after the shear force in the contact surface overpowers the frictional force. After the shear force in the contact surpasses the frictional force, the plates will slip and lose the initial rigidity which in turn will lead to more plastic deformation in the plates. With the static analysis this point of slipping is a very fine line in the loading of the structure. In dynamic analysis the frictional contact is calculated separately for all time increments so the change in rigidity is not as significant.

An interesting observation can also be made from the static average loading results. It is very clear that these do not contribute large enough load to reach satisfactory deformation values in the higher speed impacts. In hindsight, this must be also because the average loading over

40 ms is also only applicable for the 1.0 m/s impacts. This is due to the 40 ms time interval being based on the EN 81-50 standard which defines its' design requirements to the 1.0 m/s impact. This same requirement for higher impact speed would possibly need to have smaller time range for the average. In Figure 36 is presented the definition of the 40ms interval.

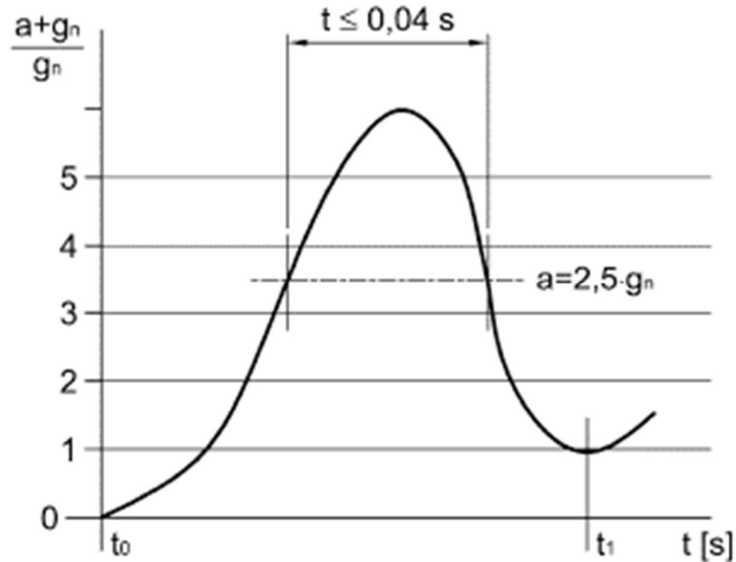


Figure 36. 40 ms requirement definition (EN 81-50 2020, p. 27).

The EN 81-50 standard defines the 40 ms time interval from the peak of the acceleration in the 1.0 m/s impact. For higher speed impacts the peak of the acceleration in the impact would show more sharper curve resulting in a shorter time range for the average, which is the reason that the average loads are too small in this research calculated with the 40 ms range. When comparing the maximum load results to the average load results it could be estimated that a good load case for static analysis would be somewhere in between presented maximum and static load case ranges. A good static load case would have slightly higher loading than the presented average load cases and lower loading than the maximum load cases, which would indicate that more correct average would yield better results.

The dynamic models with the initial velocity and the standard earth gravity loading seem to produce similar results in all model configurations. They overall provide larger deformation results than the experimental drop tests, but the trend seems to be similar in all cases, except for the 2.5 m/s model of the strong plate. In the strong plate 2.5 m/s model the difference to

the result trend comes from obvious deformations in the geometry of lower parts of the model. The top plate of the beam deforms significantly and is affecting the other top parts of the model. This is presented in Figure 37.

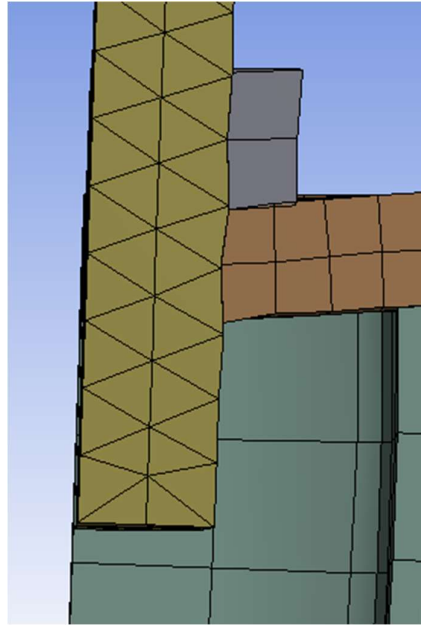


Figure 37. Deformation in the top plate, 2.5 m/s dynamic ($v_0 + g$) model.

This deformation in the top plate of the extension will take away from the deformation in the buffer plate. In experimental testing the top plate of the beam had no visual plastic deformation, but the structure overall was possibly very close to significant failures. This would indicate that the dynamic models with initial velocity and standard earth gravity, provide slightly higher loads than in experimental data with these analysis configurations. Which in turn result in higher deformations than in the drop test specimens, but the scale of the deformations should also be considered when evaluating the applicability of the method.

When compared in percentual difference the difference seems very high, but when compared in terms of the magnitude, the differences are only in the range of few millimeters. In the 1.75 m/s impacts the strong plate has approximately 1.6 mm difference to the drop test and the weak plate has slightly more deformation of approximately 2.9 mm compared to the drop test as it should have, because the structure is weaker.

The equivalent von Mises stress concentrations were not a point of focus in this thesis, but the concentrations point out distinct problems with the higher speed impact analyzes especially in the static maximum load cases and with the impact speed of 2.5 m/s. In these models, large stress concentrations close to, or even higher than the ultimate strength limit of the steel are visible. As previously mentioned, as a material model in ANSYS reaches the ultimate strength limit, the analysis will from that point onward treat the material as fully plastic, which in turn will result to, in some extent unnecessarily large deformations. In the 2.5 m/s dynamic model, large concentrations of high stress concentrations also form in the lower part of the structure which result in the failure of the top plate of the beam as presented in Figure 37 above.

6.2 Applicability to buffer extension design

From the observations regarding 1.0 m/s impacts it can be confidently said that all the tested FE-analysis methods would give reasonable approximations on deformations in the extension structure. However, the most efficient method for defining the load case is the impact factor load calculation. With it, there is no need to do any additional testing to determine the load for the static analysis, the load can simply be calculated from the formula. The static analysis is much simpler to setup and faster to analyze than the dynamic models. The results also should give very close to equal results as in the experimental tests.

For more higher speed impacts, the definition of the best methods is not that clear. Figure 38 was created based on the values in Table 12 to more clearly indicate the trend of stability of the different analysis methods in terms of magnitude difference. In Figure 38 is presented the trend of differences in the results of the analyses compared to the experimental tests. A negative value signifies less plastic deformation in an analysis than in the experimental test and positive value signifies a larger plastic deformation.

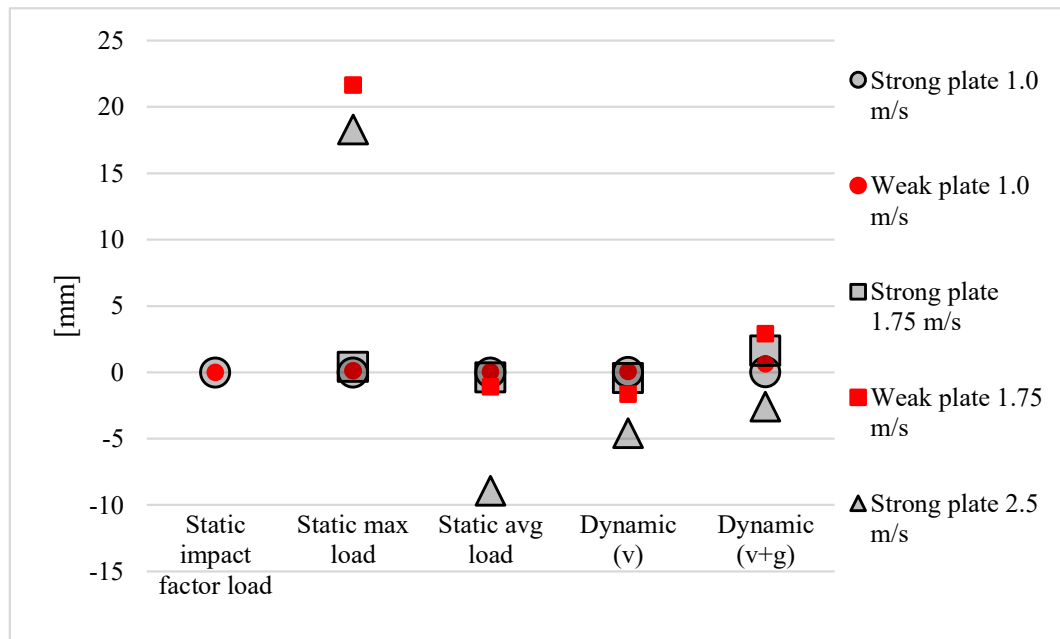


Figure 38. Trend of magnitude difference in deformation results of different analysis methods compared to drop test results.

As previously mentioned, all methods for 1.0 m/s impacts are very close to the results of drop tests. The static maximum loading is also clearly too large for all higher speeds, especially with the weak plate configuration, and the static average as well as the dynamic loading with only the initial speed are too small. The dynamic models with initial velocity and standard earth gravity provide slightly higher deformation results than the drop tests but they are the most stable of the methods with also the weak plate configuration. In the previous bar diagrams the differences in the results look very large, but the difference in magnitude is more comprehensible when applied in real-life.

The difference in deformations in experimental results is not very large, for example in the strong plate 1.75 m/s impact it is only 1.5 mm and in the weak plate the difference is 2.9 mm. Which is why the dynamic analysis would be the most applicable method for higher speed impacts, the loading implies a factor of safety of approximately 2-4. This method could be used in design process of new extension structures if higher impact speeds need to be evaluated. If a designed structure can maintain integrity with this loading, it should also in experimental tests fit the requirements. The safety factors might seem very large, but the structures overall are not very large assemblies which means that material saving achieved with lower safety factors would be relatively small. With all this in mind, the dynamic

analysis could be applied to buffer extension design with impacts speeds at least up to 1.75 m/s. With impact speeds higher than this the loading in the analysis is too large respect to the material models used in this research.

For the highest impact speed of 2.5 m/s no valid method for evaluation was found. The dynamic load for the 2.5 m/s impact is following the same trend as with the other dynamic models but the high loading causes significant deformations in buffer plate and in the bottom part of the structure as well. With more accurate material models the analysis could be possibly improved and the results would be closer to the same levels as with the other high-speed impacts.

6.3 Reliability, validity and sensitivity aspects

Biggest problems for the numerical accuracy in the scope of this thesis was the material models. Firstly, the non-linear material model for steel is very simple, only including the yield point for the plastic deformation and the ultimate strength after which in solver the material behaves as fully plastic. Proper material model for the steel would not be linearly plastic after yielding, especially just before ultimate strength is reached the strain hardening would be significantly more non-linear than in this linear model, and after ultimate strength there would be some necking of the steel rather than it being fully plastic. Even bigger factor of inaccuracy in the models was the PU-material model. The hyper-elastic material model is suitable for depicting the stress strain behavior, but the data from which this material model was generated was very limited. The manufacturer provided only force deflection diagrams from which the true stress strain behavior was estimated, no accurate data was used to create the hyper-elastic material model.

The lack of an accurate material model for the PU can also be seen in the speed diagrams of the dynamic models. The overall decrease in speed is achieved in very close to the same time with the dynamic loading including initial speed and gravity as in the experimental tests, but the decrease in speed is more rapid in the beginning of the impact in the experimental tests. This inaccuracy affects the deformation results in the dynamic analysis, because in the experimental results a large portion of the energy of the impact is dissipated in the beginning of the impact. The utilized material model does not have a sharp enough hardening in the beginning part of the stress-strain curve to achieve this.

Second biggest problem for the numerical methods was modeling of the frictional contacts, especially in the dynamic models. The accuracy of the frictional contacts in the static models mainly only depend on the correct setting of the static frictional coefficient. However, in the dynamic models the contacts are far more difficult. The biggest problem with the contacts was the contact between the plate and the PU-buffer. The hyper-elastic PU material will after deforming enough translationally reach the plate edge and slip over the edge, and this point of slipping over the edge is very difficult for the simulation. If the PU would be squeezed between two parallel smooth planes the contact would be simpler, but in this case when the deformation goes over the plate edge the elements do not recognize the contact properly. Smaller mesh size would probably help with this but that will also drastically increase the analysis time. In addition to this the frictional contacts of steel to steel have some inaccuracies with the static friction coefficient. ANSYS has also an option for dynamic friction coefficient which could be applied after the initial frictional slipping, but this would also require a decay constant for the transition between the static and dynamic coefficients which would be needed to be measured in testing. In addition to this the simplifications in geometry modeling undisputedly have an effect of the final results, but this kind of simplification is very normal to do to accomplish more easier modeling process. The mesh size was overall very coarse in the models which will result in more inaccurate results, it would be beneficial to have at least 4 elements through the thickness of the plates to get better stress distribution output. In dynamic models also the time step sizes which are as default determined by the element size effect the accuracy of the analysis, but they also have inevitable influence on the analysis solving time. With the settings used in this analysis the longest calculation times were close to 8 hours, there is some possibility for time step size decrease, but the calculation time needs to be kept reasonable. Furthermore, it is also evident that with numerical method such as FE-analysis the results it provides are always approximates.

Smaller factors regarding the sensitivity and the reliability of the results have to do with for example the measurement of the deformations in the test specimen. Deformation is most visible in the plates but there might be some small deformation in the other parts of the structure especially in the high-speed impact test which cannot be noticed visually. In addition to this the measurement method of the plates was very simple. The measurements were done with a mechanical vernier caliper, and even with a calibrated digital vernier

caliper and a more structured measuring environment, more accurate results could be achieved, but in the terms of the scope of this thesis this was not necessary.

The PU-buffer in the FE-models deforms very much but this is also true in the experimental tests, especially with the higher speed impacts. A major failure of the polyurethane can be very close in the high-speed experimental tests, but at least in these tests the PU endured the impacts without tragic failures. However, in real-life impact situation the functionality of the buffer should be verified and to assure safe operation and the PU should be changed to a new one. In addition to this it needs to be stated clearly that the PU-buffers designed according to EN 81-20 and EN 81-50 standards, do not ensure safe impacts in higher speeds than the specified 1.0 m/s impact.

Overall, inside the scope of this thesis the validity of the results is sufficient. With the applied methods the results are in the range of few millimeters from the experimental results, which is suitable for design applications and with some improvements even more accurate results are possible.

6.4 Suggestions for improvements

The biggest improvement for further research in the future has to do with the previously mentioned biggest problems. Firstly, the most beneficial improvement for the FE-analysis would be more accurate material models, especially for the PU material. This would require measurements of the material in question, for the PU this would mean proper volumetric testing and stress-strain data for axial and translational directions. Axial data most desirably would need to be tensile stress-strain data, hyper-elastic material models in Ansys Workbench are usually created with tensile stress-strain data. Secondly, the same proper definitions for the steel material model could be done. Tensile stress-strain data could be used to create an accurate multilinear material model for the steel which would yield more accurate results. Finally, some measurements of the frictional contacts could be done to determine accurate frictional coefficient for PU on steel contact. In addition to this, measurements to determine the frictional decay for steel-on-steel contacts could be made so the dynamic friction coefficient could be utilized.

Some smaller optimizations would also be reasonably easy to do. The mesh size could be made finer at least in the static models with which the long calculation times are not a problem. If possible, more elements through the thickness of the geometries in the model could be used to achieve more accurate stress distribution. In the dynamic models some mesh refinement is still possible without slowing down the calculation times significantly. Also, a slightly smaller time step increments could be used in the dynamic analysis.

In results analysis it was discussed that the 40 ms average might be too large range for averaging the forces for higher impact speeds than 1.0 m/s. Further investigation could be made to find out if a smaller range for the average interval would lead to better results, the result data would suggest that the optimal forces for static loading would be somewhere in between the maximum loading and the currently used 40 ms average loading. A smaller range for averaging the force would lead to a slightly higher force which could be better for the static analysis than the loading cases presented in this thesis.

In addition to these, a more thorough investigation regarding the analytical model presented in the thesis could be carried out to understand the impact phenomena in this frame of work. This could provide more knowledge on how to simulate the deformations in a system which consists of a buffer and a steel structure. If the analytical model proves to be accurate it could be also used in evaluation of new buffer extension structure designs.

Overall, even though good propositions for analysis of the higher speed impacts were made from the results in this thesis, the same methods would still need to be tested in a wider range of buffer extension geometries. The other buffer extension designs are generally more simple than the evaluated structure in this thesis, which would suggest that applying the methods should be straightforward. Certainly, the modeling process is also easier to execute now that some good initial settings for the dynamic analysis have been found.

7 CONCLUSIONS

This thesis focused on finding out the best possible methods of evaluating elevator buffer extension structures under impact loading. The goal of the thesis was to find out if static FE-analysis is applicable to normal design requirements for the buffers with 1.0 m/s impacts or does the analysis need dynamic loading in the FE-analysis to approximate proper loading of the structure. This was done because the standards do not provide guidance to calculations. The additional objective of this thesis was to find the best possible method of evaluating impacts with higher than 1.0 m/s impact speeds.

The assessment of the methods was done by selecting a buffer extension structure geometry for evaluation with two different configurations and analyzing the structures under different impact speed loadings with static and dynamic FE-analysis. For static analysis three different types of loading for all impact speeds were created to represent the impact loading on the structure. With the dynamic analysis loading can be created as mass impacting the structure, which means that no additional calculation of loads is needed. For the dynamic analysis two different types of loading was tested, one with initial velocity and other with initial velocity and standard earth gravity. Experimental drop test data was used as the reference to which these numerical methods were compared to.

From the results it was possible to clarify that all presented methods would be applicable for 1.0 m/s impact speed evaluation of the structure. The most practical method of these for design purposes is the impact factor loading, with which no additional measurements need to be done for approximating the loading. An accurate approximation of the impact load in 1.0 m/s impact can be done by a simple formula. The static FE-models are also faster to implement and solve than the dynamic models. For the higher impact speeds a sufficient method was found to analyze impact speeds up to 1.75 m/s. A dynamic FE-model with initial velocity and standard earth gravity as loading for the impact mass will provide adequate results. With the applied material models the loads were slightly too large compared to experimental results, but the magnitude of the difference in results would still be functional for design purposes.

Suggestions for further development of the methods could also be introduced. It was found out that one of the biggest factors in analysis accuracy were the relatively simple material models. Material models created from realistic testing data would result in more accurate approximation of the deformations in the structures. Especially proper testing for hyper-elastic material model would help, even if the buffer material is not kept as absolutely the same. One of the biggest problems during the dynamic simulation was the contact properties in frictional contacts, measurements for more accurate definition of friction coefficient could help negate at least the impact to the result accuracy.

Overall, the research was successful in fulfilling the set goals and providing more insight to simulating this type of phenomena which will also help in future developing these methods further. Before utilizing these methods in buffer extension design these methods need to be applied to also different types of buffer extension structures available, to assess if the methods are applicable in larger scope. This assessment should be reasonably simple to execute with the presented configurations of FE-models.

LIST OF REFERENCES

Ciortan, I., Giurgiu, I. & Pupăză, C. 2014. Passive Mitigation Solutions Using Explicit Dynamics Simulation. Proceedings of the Romanian Academy. Series A. Vol. 15. 3. Pp. 262-271.

Cruz Gomez, M.A., Gallardo-Hernandez, E.A., Vire Torres, M. & Peña Bautista, A. 2013. Rubber Steel Friction in Contaminated Contacts. Wear of Materials. 1-2. Vol. 302. Pp. 1421-1425.

Engineering Library 2022. [Engineering Library www-page]. [Referenced 27.6.2022]. Available: <https://www.engineeringlibrary.org/reference/coefficient-of-friction>

Hyper Textbook 2022. [Hyper Textbook www-page]. [Referenced 27.6.2022]. Available: <https://hypertextbook.com/facts/2005/steel.shtml>

Kim, N. 2015. Introduction to Nonlinear Finite Element Analysis. Springer. 430 p.

Li, R. 2021. Research on Application of Finite Element Method in Static Analysis. Journal of physics. Conference series. Vol. 1802. 4. 4 p.

Ling, Y. 1996. Uniaxial True Stress-Strain after Necking. AMP Journal of Technology. Vol. 5. Pp. 37-48.

Lozzi, A. & Briozzo, P. 2000. Failure of an inclined elevator. Proceedings of the Institution of Mechanical Engineers: Journal of Mechanical Engineering Science. Part C. Vol. 214. 2. Pp. 323-333.

Meram, A. 2019. Dynamic characterization of elastomer buffer under impact loading by low-velocity drop test method. Polymer testing. Vol. 79. 10. 10 p.

Mirables, R., Cuartero, J. & Castejon, L. 2013. Biomechanical Response and Behavior of Users under Emergency Buffer Crash. Advances in mechanical engineering. Vol. 5. 1. 10 p.

Thilmany, J. 2013. High standards as elevators advance so do their safety codes. *Mechanical engineering*. New York. Volume 135. Pp. 46-49.

EN 1993-1-1, 2005. Eurocode 3: Design of steel structures – Part 1-1: General rules and rules for buildings. European Committee for Standardization. 91 p.

EN 81-20, 2020. Safety rules for the construction and installation of lifts. Lifts for the transport of persons and goods. Part 20: Passenger and goods passenger lifts. 2nd edition. European Committee for Standardization. 158 p.

EN 81-50, 2020. Safety rules for the construction and installation of lifts. Examinations and tests. Part 50: Design rules, calculations, examinations and tests of lift components. 2nd edition. European Committee for Standardization. 110 p.

Yarar, E., Erturk, A. T., Karabay, S. 2021. Dynamic Finite Element Analysis on Single Impact Plastic Deformation Behavior Induced by SMAT Process in 7075-T6 Aluminum Alloy. *Metals and Materials International*. 27. Pp. 2600-2613.

Wang, Y., Zhang, G., Ma, C., Yang, K., Zhang, Z. & Ren, Z. 2019. Explicit Dynamics Simulation of High-Speed Railway Bearing Based On ANSYS/LS-DYNA. *IOP conference series. Materials Science and Engineering*. Vol. 612. 11.